VERIFICATION & VALIDATION

TIME-VARYING DISCHARGE MODEL

DATE: December 2023

Reference to part of this report which may lead to misinterpretation is not permissible.

No.	Date	Reason for Issue	Prepared by	Verified by	Approved by
1	Feb 2010	First issue	Jan F. Stene		
2	Oct 2017	Phast 8.0	Jan Stene		
3	May 2021	Apply new template			
4	July 2022	Version update	David Worthington		

Date: December 2023

Prepared by: Digital Solutions at DNV

ABSTRACT

This report documents verification and validation work carried out for the time-varying discharge model TVDI during the development of Phast 6.6. Note that this version of the TVDI model is present in Phast 7.22 and earlier, while Phast 8.0 and later has a new version of the TVDI model. All versions of Safeti Offshore includes the new TVDI model.

The verification includes the following scenarios:

- Leak through the orifice of a vessel with sub-cooled water
  - with and without pressurized vapour space
  - usage of all available vessel shapes
- Leak through the orifice of a pressurized gas vessel

The validation includes these scenarios:

- Three cases of blowdown of pressurized hydrocarbon vessels
- Blowdown of an LPG cylinder through a long pipe attached to the vessel

Table of contents

1 INTRODUCTION

NB! Phast and Safeti 8.0 and later versions contain a new version of the TVDI model. The results presented in this document are for the old model present in version 7.22 and earlier. A similar verification and validation document will in the future be provided for the new TVDI model.

The purpose of this document is to present verification and validation results for the **t**ime-**v**arying **di**scharge model (TVDI) in Phast[i]. TVDI contains models for calculating the continuous time-varying discharge from a vessel with / without an attached pipe, and three types of failure / release scenarios may be simulated: (a) Leaks from the main process vessel; (b) Full bore rupture of connected pipe; (c) Discharge from pressure relieving devices (e.g. bursting discs or pressure relief valve). Detailed information about the model and its theory can be found in the accompanying theory manual TVDI_theory.docx.

Some further TVDI validation can be found in Chapter 4 of the validation document for the unified dispersion model (UDM).[1]

1.1 Background and organization

Planned upgrade of the TVDI model made it necessary to first properly document and understand the existing model. The first stage of this process included the creation of the theory manual TVDI_theory.doc. The second stage is then to *verify* that there is correspondence between the theory as extracted from the code and the actual results produced by the code. The third stage would then be to *validate* the model, i.e. to compare results predicted by the model with corresponding experimental data to assess how well the model actually describes real physical scenarios.

This document is split into two main parts. The first part deals with the verification of the TVDI model, while the second part deals with the validation. As the TVDI model currently consists of two separate sub-models, each of the two main parts is further divided into two sections: one section covering the liquid/two-phase sub-model, and one section covering the pure gas sub-model.

[i] Unless specifically stated, Phast 6.6 has been used to obtain the results in this report.

2. VERIFICATION – LIQUID AND TWO-PHASE RELEASES

2.1 Introduction

This sub-model simulates the transient depressurisation process following loss of containment from a multi-phase (vapour-liquid) vessel.

Three types of release scenarios involving single (vapour/liquid) or two-phase flow can be simulated. These are:

- Leaks from the main process vessel.
- Full bore rupture of connected pipework.
- Discharge from pressure relieving devices (e.g. bursting discs or pressure relief valve).

The multi-phase vessel model is illustrated in Figure 1.

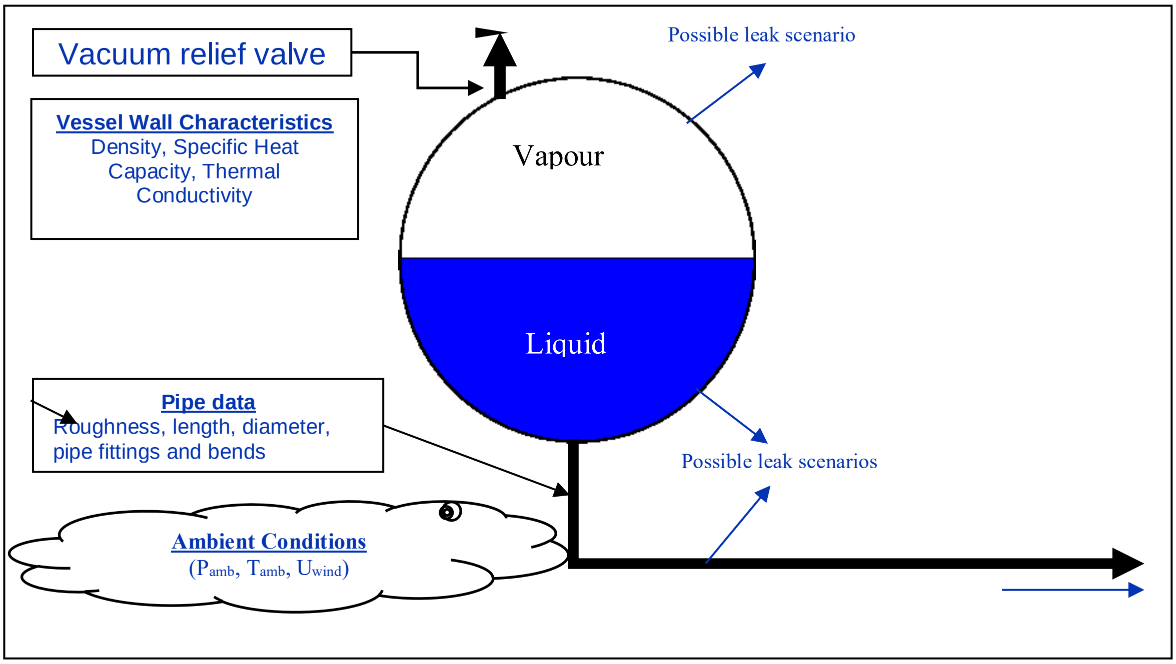

Figure 1: Current version of TVDI in Phast 6.6

2.1.1 Scope and Methods

The discharge model TVDI is applied to releases of water from both unpressurised and pressurised vessels of all applicable geometry types. The results are then compared to analytical results based on the Bernoulli equation - see Section 2.3 for details.

Some relevant background theory for the relevant analytical formulas is first presented in Section 2.2, and an overview of software that could potential be used for verification is presented as well.

Some of the analytical formulations are ordinary differential equations that are solved using an explicit fourth-order Runge-Kutta method in an Excel spreadsheet environment. Excel has also been used to actually compare analytical and TVDI results graphically.

2.1.2 Omissions

Current omissions:

- Release from attached pipes
- Two-phase releases

2.2 Verification options and possibilities

2.2.1 Analytical verification

Section 15.1.10 in Lees[2] contains analytical expressions for the time for discharge for the cases of a liquid release from a vertical cylindrical vessel with finite imposed pressure [Equation (15.1.98)] and a spherical vessel with no imposed pressure [Equation (15.1.102)]. Similar formulas are provided in Figure 2.8 in Section 2.3.5.3 in the Yellow Book[3]. A recent paper by Hissong[4] also gives formulas for the time-dependent discharge rate for spherical and membrane tanks. TVDI could be verified against these formulas.

2.2.2 Orifice leaks for liquids:

- Flow rate equations:

$$general: \frac{dm}{dt} = C_d\ A_{ou}\ \rho_{od}\ u_{od}\ ,\ u_{od} = \sqrt{2(h_{st} - h_{od})} \qquad (many\ other\ 2-phase\ models!]$$

$$incompressible\ \ liquid: \frac{dm}{dt} = C_d\ A_{ou}\ \rho\sqrt{\frac{2(P_{st} - P_{od})}{\rho}} \qquad (Bernouilli)$$

With

T = temperature (K)	p = pressure (Pa)
ρ = density (kg/m^3)	u = velocity (m/s)
h = enthalpy (J/kg)	M_w= molecular weight (kg/kmol)
γ = ratio of specific heats	R = gas constant = 8314 (J/kg/kmol)

2.2.3 Time-varying Bernoulli equation for sub-cooled liquids

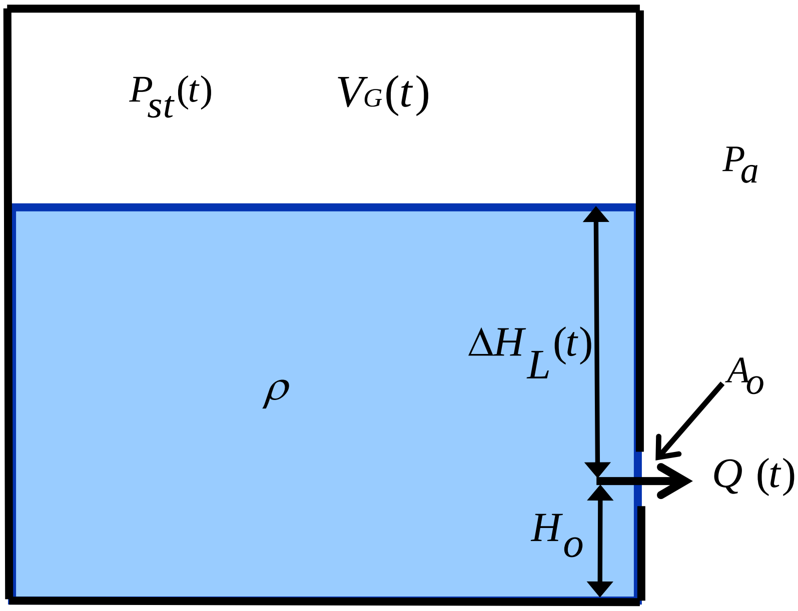

Figure 2: Schematic orifice leak from a vessel.

Assuming a sub-cooled liquid leak from a vessel orifice and applying energy conservation, the Bernoulli equation yields[4]

$$Q(t) = C_D \ A_o \ \rho \sqrt{2\left(\frac{P_{st}(t) - P_a}{\rho} + g\Delta H_L(t)\right)} \qquad \textbf{(1)}$$

This may equivalently be expressed as[5]

$$\frac{d\left(\Delta H_L(t)\right)}{dt} = -\frac{C_D \ A_o}{A(t)} \sqrt{2\left(\frac{P_{st}(t) - P_a}{\rho} + g\Delta H_L(t)\right)} \qquad \textbf{(2)}$$

where

$$Q(t) = -\rho A(t) \frac{d(\Delta H_L(t))}{dt} \qquad \textbf{(3)}$$

In general one may thus obtain the flow rate from Equation (3) after first solving the ODE (2) for the liquid head ΔH_L.

Unpressurised vessels with constant cross-sectional area
Assuming that the storage tank is vented to the atmosphere such that the pressure is equal to the atmospheric pressure, and that the tank has a constant cross-sectional area A , Equation (2) simplifies to the separable ODE

$$\frac{d(\Delta H_L(t))}{\sqrt{\Delta H_L(t)}} = -C_D \ \frac{A_o}{A} \sqrt{2g} dt \qquad \textbf{(4)}$$

with the following analytical solution:

$$\Delta H_L(t) = \left[\sqrt{\Delta H_L(0)} - \frac{C_D A_o \sqrt{2g}}{2A} t \right]^2 \quad \textbf{(5)}$$

Substituting Equation (5) into Equation (1) then yields this mass release rate as a function of time:

$$Q(t) = C_D \; A_o \; \rho \left(\sqrt{2g\Delta H_L(0)} - \frac{C_D A_o g}{A} t \right) \quad \textbf{(6)}$$

The release is complete when the mass release rate is zero, so the release duration can be found by:

$$t_{rel} = \frac{A\sqrt{2g\Delta H_L(0)}}{A_o C_D g} \quad \textbf{(7)}$$

The relevant tank types with constant cross-sectional area are cubiodal tank with area

$$A = L_{\text{tank}} W_{\text{tank}} \quad \textbf{(8)}$$

and vertical cylinder with area

$$A = \pi r_{\text{tank}}^2 . \quad \textbf{(9)}$$

Unpressurised vessels with non-constant cross-sectional area
To be able to solve Equation (2) we need to express the cross-sectional area of the tank at a given liquid height. For the relevant tank types we then have[5]:

Spherical tank:

$$A(\Delta H_L) = \pi (H_o + \Delta H_L)(2r_{\text{tank}} - H_o - \Delta H_L) \quad \textbf{(10)}$$

Horizontal cylinder:

$$A(\Delta H_L) = 2L_{\text{tank}} \sqrt{(\mathrm{H_o} + \Delta \mathrm{H_L})(2\mathrm{r_{tank}} - \mathrm{H_o} - \Delta \mathrm{H_L})} \quad \textbf{(11)}$$

The resulting ODE's are solved numerically by an explicit fourth-order Runge-Kutta method (ERK4). The associated drainage times are then given by:

Sphere:

$$t_{rel} = \frac{\pi\sqrt{2g}}{A_o C_D g} \left[\frac{2}{3} \Delta H_L^{3/2}(0)(r_{\text{tank}} - H_o) - \frac{1}{5} \Delta H_L^{5/2}(0) + H_o \Delta H_L^{1/2}(0)(2r_{\text{tank}} - H_o) \right] \quad \textbf{(12)}$$

Horizontal cylinder:

$$t_{rel} = \frac{\sqrt{2g} L_{\text{tank}}}{A_o C_D g} \int_{H_o + \Delta H_L(0)}^{H_o} \sqrt{\frac{1}{\Delta \mathrm{H_L}}} (\mathrm{H_o} + \Delta \mathrm{H_L})(2\mathrm{r_{tank}} - \mathrm{H_o} - \Delta \mathrm{H_L}) d(\Delta \mathrm{H_L}). \quad \textbf{(13)}$$

Pressurised vessels
The situation is more complex when assuming that the liquid is initially pressurised. We no longer assume that the tank has a vent to the atmosphere, but rather that there is a vacuum relief valve in the tank that ensures that the tank pressure does not drop below the ambient pressure. Assuming an ideal gas and isothermal expansion, the ideal gas law yields

$$p_{st}(\Delta H_L)V_G(\Delta H_L) = p_{st}(\Delta H_L(0))V_G(\Delta H_L(0)), \quad \textbf{(14)}$$

Taking the vacuum relief valve into account, we can then obtain the following expression for the tank pressure as a function of the liquid head:

$$p_{st}(\Delta H_L) = \max\left[\frac{p_{st}(\Delta H_L(0))V_G(\Delta H_L(0))}{V_G(\Delta H_L)}, P_a\right] \quad \textbf{(15)}$$

The expression for the volume of gas in the tank with orifice height H_o and given liquid head ΔH_L depends on the tank type:

Constant cross-sectional area A:

$$V_G(\Delta H_L) = A(H_{\text{tank}} - \Delta H_L - H_o) \quad \textbf{(16)}$$

Sphere:

$$V_G(\Delta H_L) = \frac{\pi}{3}\left(2r_{\text{tank}} - H_o - \Delta H_L\right)^2\left(r_{\text{tank}} + H_o + \Delta H_L\right) \quad \textbf{(17)}$$

Horizontal cylinder:

$$V_G(\Delta H_L) = L_{\text{tank}} r_{\text{tank}}^2 \cos^{-1}\left(\frac{H_o + \Delta H_L - r_{\text{tank}}}{r_{\text{tank}}}\right) - L_{\text{tank}}\left(H_o + \Delta H_L - r_{\text{tank}}\right)\sqrt{\left(H_o + \Delta H_L\right)\left(2r_{\text{tank}} - H_o - \Delta H_L\right)} \quad \textbf{(18)}$$

One can then obtain an ODE for ΔH_L by substituting Equation (15) into Equation (2) and applying the appropriate formula for the volume of gas depending on the tank type. The resulting ODE does typically not have an analytic solution in terms of elementary functions, but it can be solved numerically – for example by ERK4.

2.2.4 Verification against HYSIS/PROII/Other software packages

The list below includes a brief overview of methods and models for time-varying flow

- CFD programs:
  - ProFes – 2-phase for network of pipes (valves, pumps, multiple fluids)
  - OLGA2000–dynamic multiphase flow of oil/water/gas in wells and pipelines
- Methods for long pipelines presuming 1D pipe flow:
  - Methods presuming profiles for flow rate and pressure: Fanneløp, PHAST
  - Method of Characteristics (Wylie)

- Methods for releases from vessels:
    - Liquid and gas: simple C_d correlations
    - 2-phase: more complex (simple method, e.g. Fauske and Epstein)
- Programs specific for emergency relief and runaway reactions (DIERS) – 2-phase flow:
    - DEERS (Jaycor)
    - SAFIRE (AIChE)
    - SuperChems
- BLOWDOWN program (Imperial College):
    - complex thermodynamics, HEM 2-phase flow
    - pipe and vessel
- Recommendations from Dutch Yellow book:
    - Full-bore rupture until pressure wave hits end: Wilson's model
    - Vapour flow through small leak: Weiss model
    - 2-phase flow through full-bore rupture: generalisation of Morrow's model

2.3 Orifice Model

The TVDI model for releases from an orifice in a vessel is verified for both sub-cooled and saturated water leaks, with and without a pressurized vapour space above the liquid. All the four vessel geometries supported in TVDI are applied.

2.3.1 Method

2.3.2 Sub-cooled water release

Relevant scenario data:

- Temperature: 20° C
- Ambient pressure: 101325 Pa
- Water density:
    - 996.479 kg/m^3 at ambient pressure and at 6 atm as obtained from Phast 6.54
- Orifice height[ii]: 2.0 m
- Orifice diameter: 0.3 m
- Discharge coefficient 0.6
- Initial liquid head: 6.028268 m
- Total releasable mass: 600704.2 kg

We consider all four different tank types and two different tank pressures. Note that the dimensions of the tanks are chosen so that the initial liquid head and releasable mass remain constant across tank types.

- Tank type:
    - Rectangular tank: 10 m long, 10 m wide and 10 m high.
    - Vertical cylinder: 11.28395807 m diameter, 10 m high.
    - Spherical tank: 11.9663473 m diameter.
    - Horizontal tank: 10m diameter, 10.6883069m length.
- Tank pressure:
    - Unpressurised vessel[iii]: the pressure on top of the liquid is initially equal to the ambient pressure of 1 atm = 101325 Pa.
    - Pressurised vessel: the pressure on top of the liquid is initially equal to 6 atm = 607950 Pa.

[ii] This is the distance from the bottom of the vessel to the centre of the assumed circular orifice. Note that the orifice height specified in the TVDI spreadsheet is the height from the vessel bottom to the bottom of the assumed circular orifice, i.e. 1.85 m in this case.

[iii] The pressure on top of the liquid in the closed container is maintained at ambient pressure through the use of a vacuum relief valve in the TVDI model

This then yields a total of eight release scenarios for subcooled water. TVDI can apply the Bernoulli model for meta-stable liquid releases, and this is used here for comparison with analytical solutions of the Bernoulli equations in Section 0. However, it would be interesting to see how much the non-Bernoulli calculation method deviates, and the eight scenarios are therefore also simulated using the non-Bernoulli method.

Tank pressure	Tank type	TVDI Bernoulli	TVDI no Bernoulli	Analytical Bernoulli
Unpressurised	Rectangular box	459.5	526.9	459.5
	Vertical cylinder	459.5	526.9	459.5
	Sphere	459.5	526.9	459.5
	Horizontal cylinder	459.5	526.9	459.5
Pressurised	Rectangular box	1423.8	1632.5	1423.8
	Vertical cylinder	1423.8	1632.5	1423.8
	Sphere	1423.8	1632.5	1423.8
	Horizontal cylinder	1423.8	1632.5	1423.8

Table 1: Initial flow rate comparisons for subcooled water releases, [kg/s]

Tank pressure	Tank type	TVDI Bernoulli	TVDI no Bernoulli	Analytical Bernoulli
Unpressurised	Rectangular box	2362.7	2060.7	2614.5
	Vertical cylinder	2362.7	2060.7	2614.5
	Sphere	2071.4	1806.6	2354.9
	Horizontal cylinder	2264.8	1975.3	2540.5
Pressurised	Rectangular box	872.4	761.3	818.1
	Vertical cylinder	872.4	761.3	818.1
	Sphere	783.2	683.6	753.5
	Horizontal cylinder	1485.1	1295.5	1670.4

Table 2: Release duration comparisons for sub-cooled water releases, [s]

Tank pressure	Tank type	TVDI Bernoulli	TVDI no Bernoulli	Analytical Bernoulli
Unpressurised	Rectangular box	595129.4	595129.4	600704.2
	Vertical cylinder	595129.4	595129.4	600704.2
	Sphere	589453.4	589453.4	600704.2
	Horizontal cylinder	592857.3	592857.3	600704.2
Pressurised	Rectangular box	615651.2	615651.2	600701.4
	Vertical cylinder	615651.2	615651.2	600701.4
	Sphere	609799.5	609799.5	600699.8
	Horizontal cylinder	592857.3	592857.3	600704.3

Table 3: Total expelled mass comparisons for subcooled water releases, [kg]

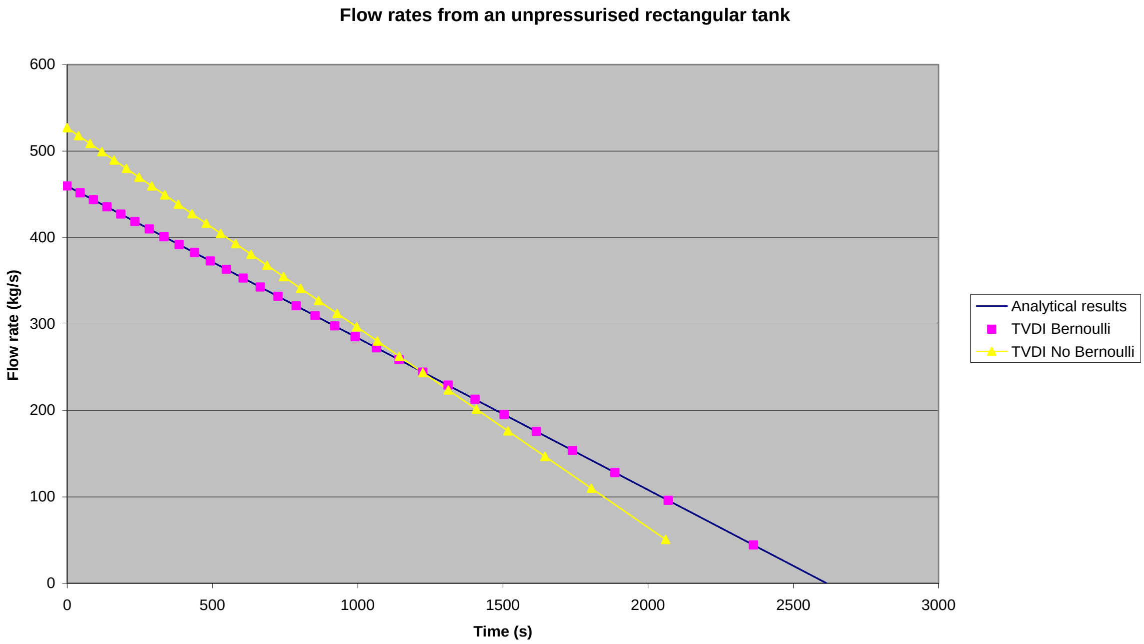

Figure 3: Comparisons of flow rates for an unpressurised rectangular tank

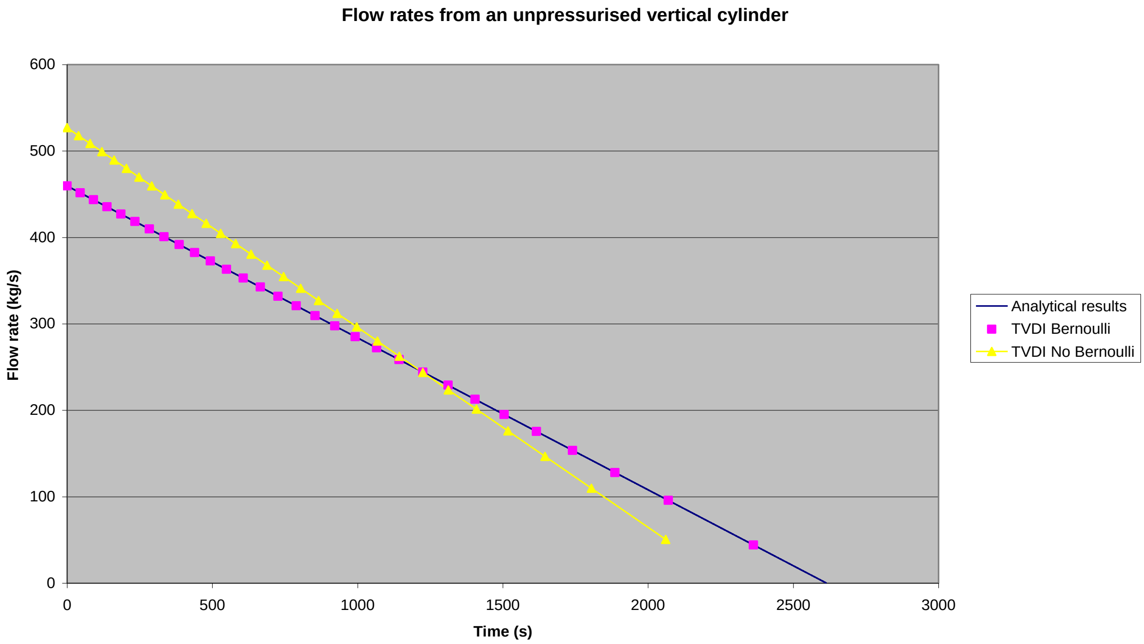

Figure 4: Comparisons of flow rates for an unpressurised vertical cylinder

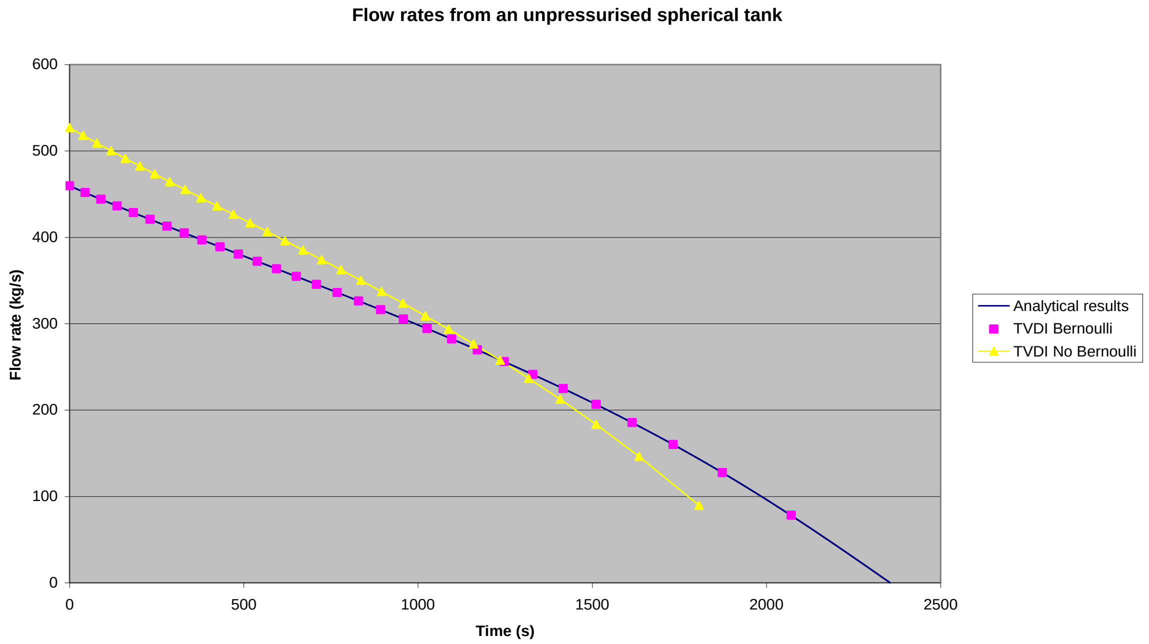

Figure 5: Comparisons of flow rates for an unpressurised spherical tank

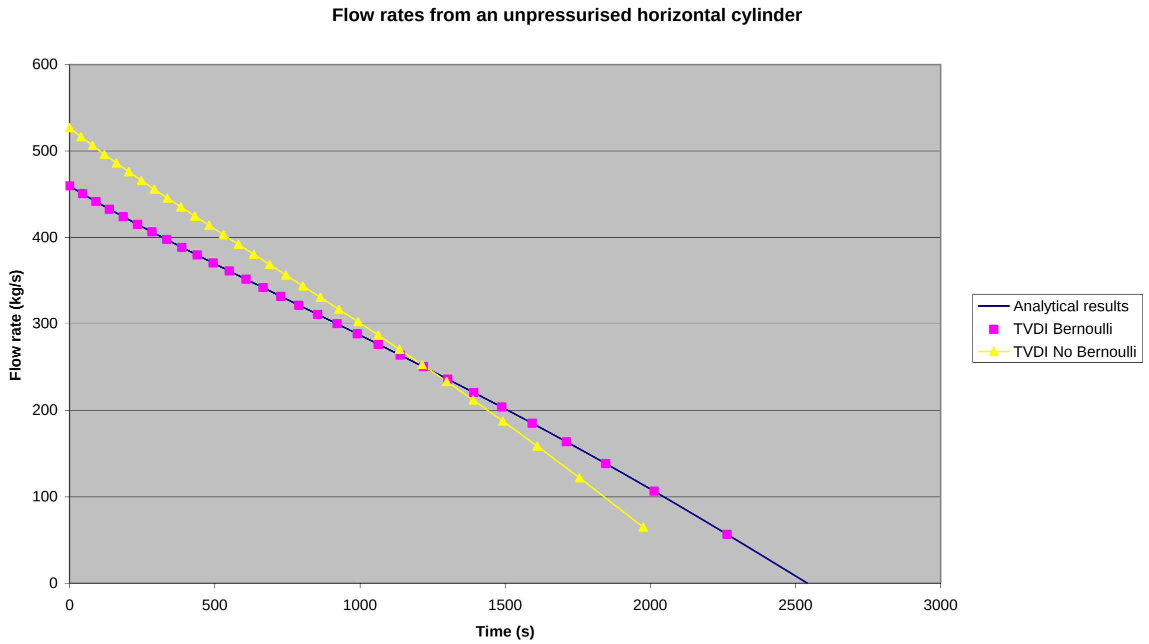

Figure 6: Comparisons of flow rates for an unpressurised horizontal cylinder

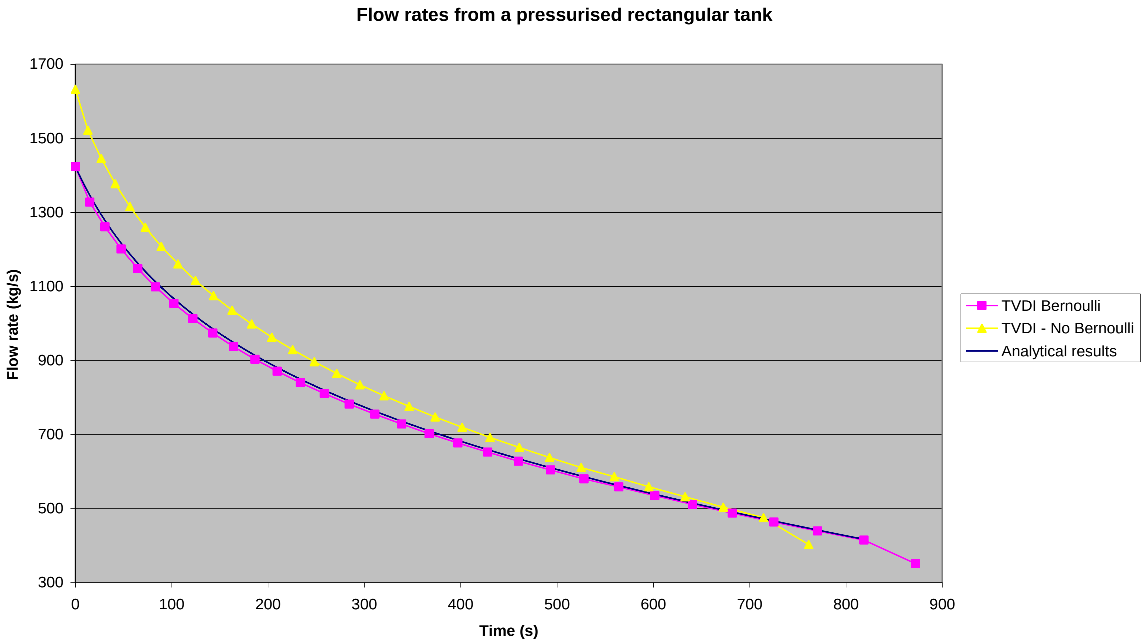

Figure 7: Comparisons of flow rates for a pressurised rectangular tank

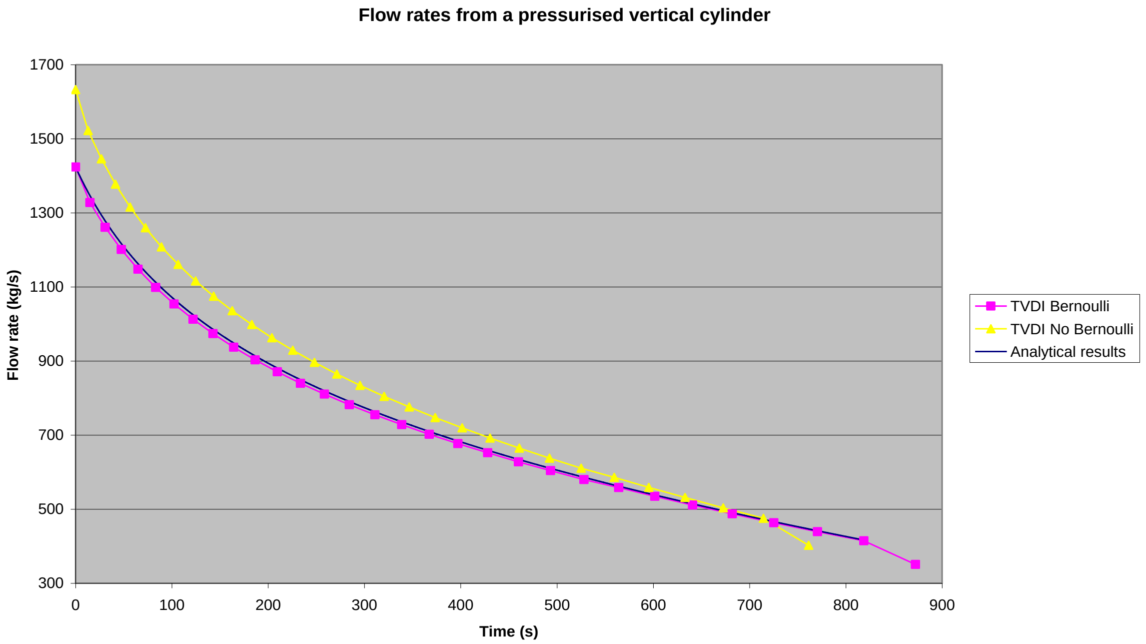

Figure 8: Comparisons of flow rates for a pressurised vertical cylinder

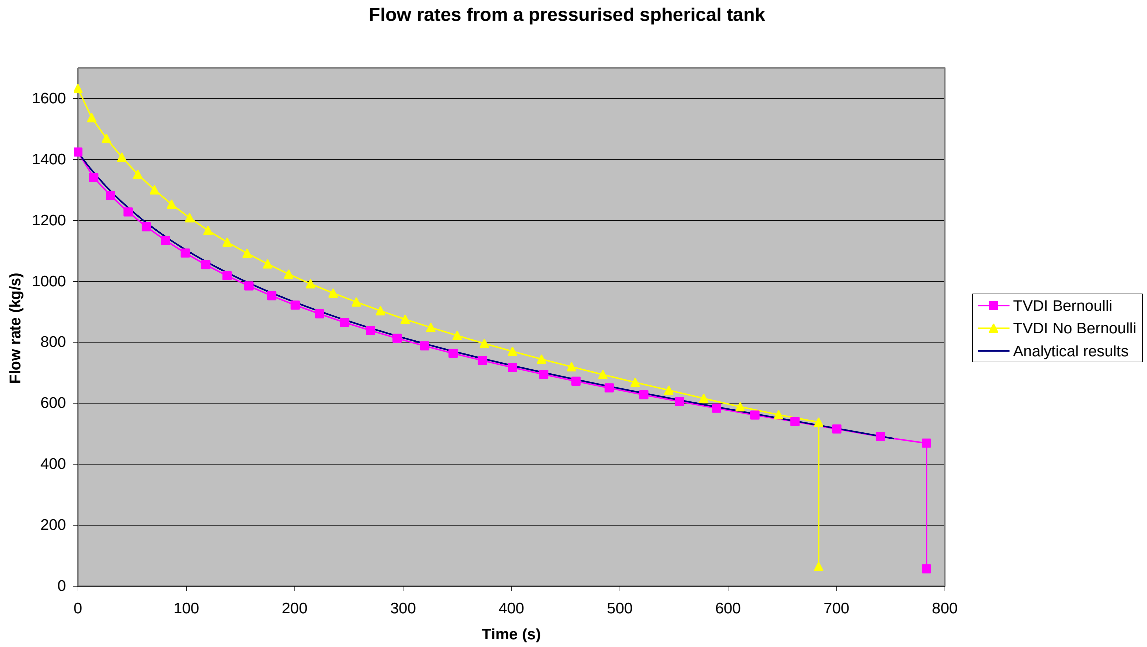

Figure 9: Comparisons of flow rates for a pressurised spherical tank

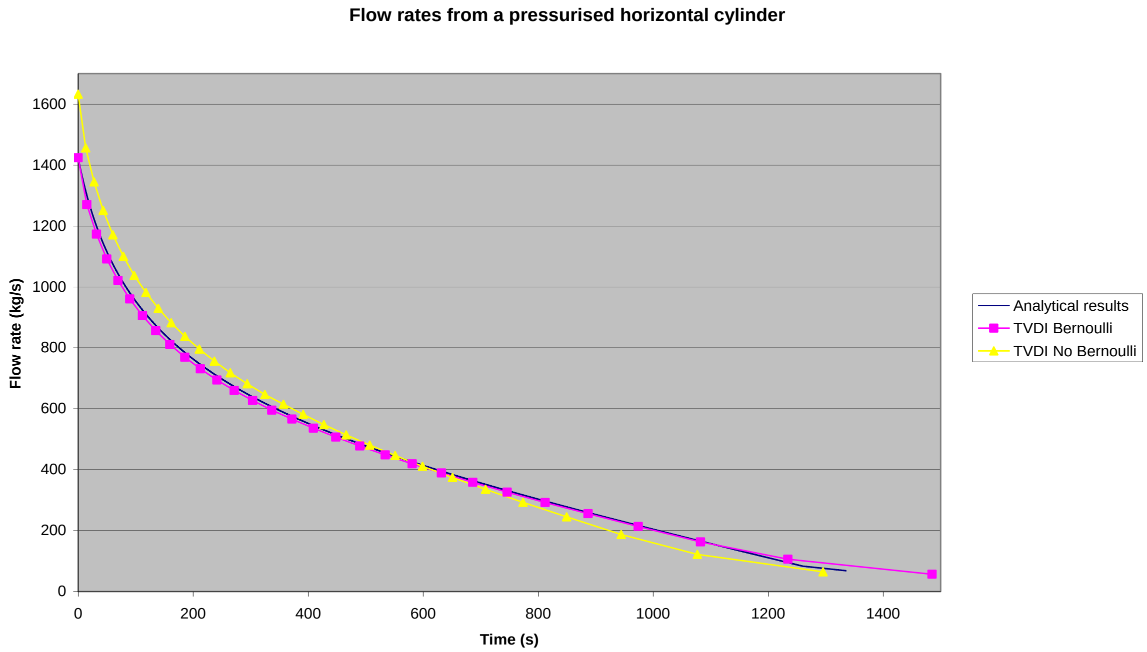

Figure 10: Comparisons of flow rates for a pressurised horizontal cylinder

2.3.3 Findings for sub-cooled water release

It is first worth pointing out the differences in results produced by the TVDI model with and without the application of the Bernoulli option. Without the Bernoulli option, the release rates are generally higher with correspondingly shorter release durations. In the remainder of this section, a comparison between analytical results and TVDI with the Bernoulli option will be considered.

Unpressurised releases
The graphs comparing analytical and TVDI predicted flow rates in Figure 3 to Figure 6 match perfectly well, and
Table 1 also show that these flow rates are identical initially. However,
Table 2 shows that TVDI predicts release durations roughly 10 % shorter than the analytically computed release durations. This difference is then reflected in
Table 3 which shows that TVDI slightly under-predicts the total mass released. The under-predictions (less than 2%) are much smaller than the under-predictions of the release durations due to the small flow rates towards the end of the releases.

Pressurised releases
The immediate conclusion from Figure 7 to Figure 10 is that there is very good agreement between predicted and analytical flow rate results. As for the un-pressurized cases there are some discrepancies for the release duration, with the total released mass difference being up to 2.5%.

List of issues
- The discrepancies observed towards the end of the release may be due to differences in the termination criteria used by the TVDI model and in the analytic computations:
    - The TVDI model should evacuate liquid until the liquid level has dropped below the bottom of the orifice.
    - The analytical results are based on evacuating liquid until the liquid level is equal to the centre of the orifice. Note that the orifice area is assumed to be the area of the full circular orifice even after the liquid level has dropped below the top of the orifice.

2.3.4 Saturated water release

Relevant data:
- Temperature: 100.0178 ° C
- Ambient pressure: 101325 Pa
    - Water density: 956.681 kg/m^3 as obtained from Phast 6.54
- Orifice height[ii]: 2.0 m
- Orifice diameter: 0.3 m
- Discharge coefficient 0.6
- Initial liquid head: 6.028268 m
- Total releasable mass: 576712.9 kg

We consider all four different tank types with the tank pressure being atmospheric. Note that the dimensions of the tanks are chosen so that the initial liquid head and releasable mass remain constant across tank types.

- Tank type:
    - Rectangular tank: 10 m long, 10 m wide and 10 m high.
    - Vertical cylinder: 11.28379168 m diameter, 10 m high.
    - Spherical tank: 11.96634727 m diameter
    - Horizontal tank: 10 m diameter, 10.6883069 m length.
- Tank pressure:
    - Unpressurised vessel: the pressure on top of the liquid is initially equal to the ambient pressure of 1 atm = 101325 Pa.

This then yields a total of four saturated water release scenarios. TVDI can apply the Bernoulli model for meta-stable liquid releases, and this is used here for comparison with analytical solutions of the Bernoulli equations in Section 0. However, it would be interesting to see how much the non-Bernoulli calculation method deviates, and the scenarios are therefore also carried out using the non-Bernoulli method.

Tank pressure	Tank type	TVDI Bernoulli	TVDI no Bernoulli	Analytical Bernoulli
Unpressurised	Rectangular box	441.2	512.1	441.2
	Vertical cylinder	441.2	512.1	441.2
	Sphere	441.2	512.1	441.2
	Horizontal cylinder	441.2	512.1	441.2

Table 4: Initial flow rate comparisons for saturated water releases, [kg/s]

Tank pressure	Tank type	TVDI Bernoulli	TVDI no Bernoulli	Analytical Bernoulli
Unpressurised	Rectangular box	2497	2152	2614
	Vertical cylinder	2497	2152	2614
	Sphere	2075	1788	2355
	Horizontal cylinder	2395	2064	2540

Table 5: Release duration comparisons for saturated water releases, [s]

Tank pressure	Tank type	TVDI Bernoulli	TVDI no Bernoulli	Analytical Bernoulli
Unpressurised	Rectangular box	571361	571361	576713
	Vertical cylinder	571361	571361	576713
	Sphere	565912	565912	576713
	Horizontal cylinder	569179	569179	576713

Table 6: Total expelled mass comparisons for saturated water releases, [kg]

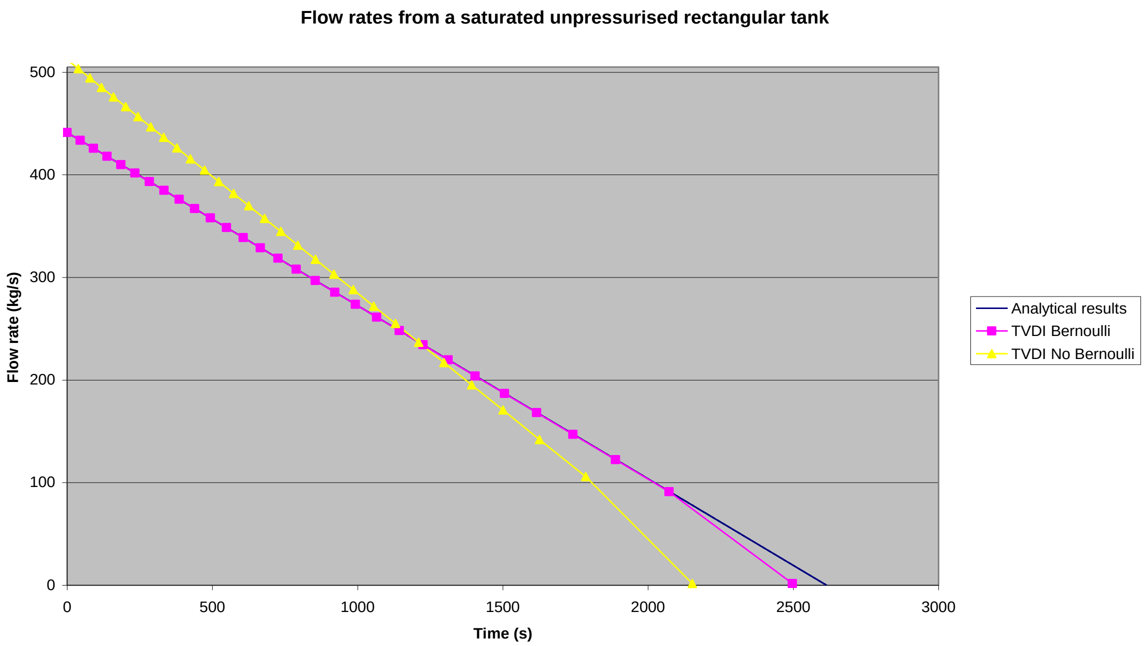

Figure 11: Comparisons of flow rates for a saturated unpressurised rectangular tank

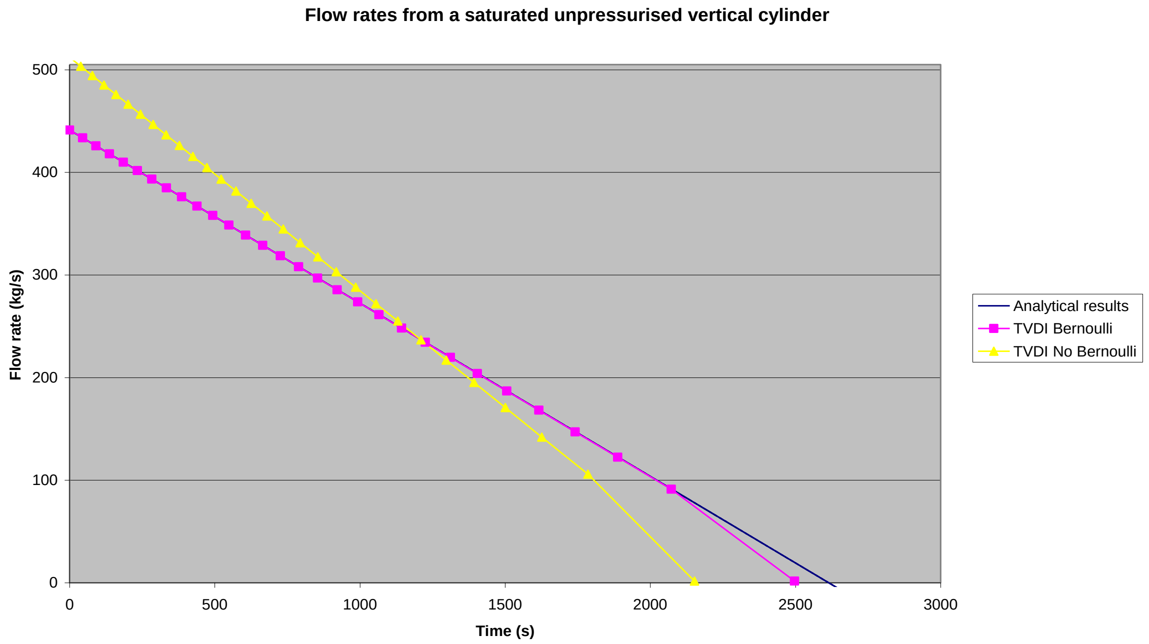

Figure 12: Comparisons of flow rates for a saturated unpressurised vertical cylinder

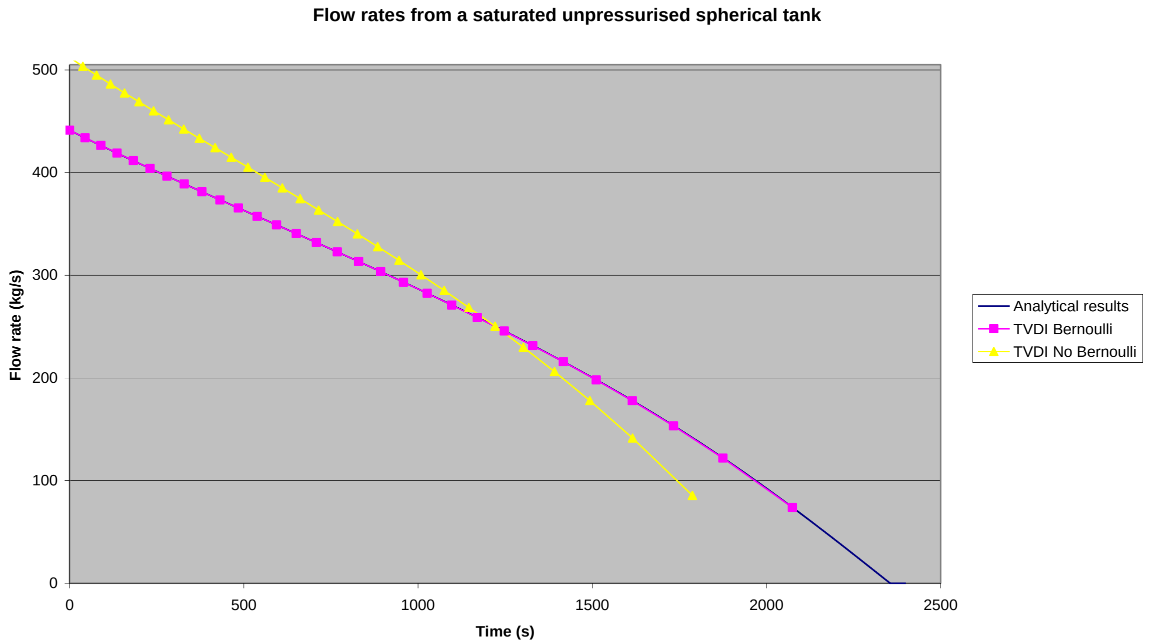

Figure 13: Comparisons of flow rates for a saturated unpressurised spherical tank

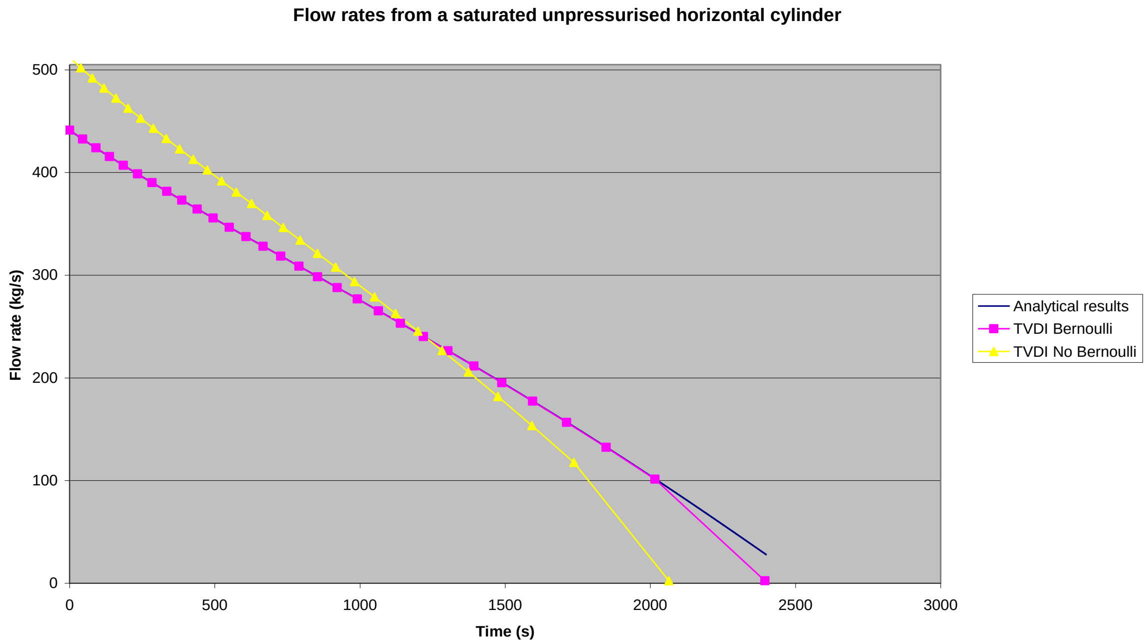

Figure 14: Comparisons of flow rates for a saturated unpressurised horizontal cylinder

2.3.5 Findings for saturated water release

Before comparing analytical and TVDI predicted results, it should be noted that analytical formulation does not take any phase changes into account. It is expected that evaporation will be particularly significant in these scenarios as the water is at boiling temperature, and TVDI does take evaporation into account. It is important to keep this fact in mind when comparing results.

The predicted flow rates by TVDI using the Bernoulli option coincide with the analytical results except at the very end of the release. This deviation may be due to different termination criteria as explained in Section 2.3.3 on the sub-cooled releases. It is also possible that the evaporation of liquid taken into account by the TVDI model yields a smaller hydrostatic head which becomes significant towards the end of the release, resulting in a smaller TVDI release rate than the analytical release rate.

3. VERIFICATION – PURE GAS RELEASES

3.1 Introduction

3.1.1 Background and Purpose

Model upgrade made it necessary to first properly document and understand the existing model, and part of this understanding is a verification exercise to see that there is correspondence between the theory extracted from the code and the actual performance by the code.

3.1.2 Scope and Methods

3.1.3 Omissions

Current omissions:

- Release from attached pipes

3.2 Verification options and possibilities

3.2.1 Analytical verification

The paper by Sallet and Palmer[6] deals with the non-steady, isentropic flow of gases from pressure vessels. In the case of choked flow, the paper contains analytic formulas for transient mass flow rates, tank pressures, temperatures and gas densities, and TVDI is verified against these formulas.

3.2.2 Orifice leaks for ideal gases

Often quoted from the literature (see e.g. Lees):

- Discharge coefficient $C_d = \dfrac{area\ of\ vena\ contracta}{area\ of\ orifice} = \dfrac{A_{od}}{A_{ou}}$
- Cd = 0.6 (sharp orifice) -1 (rounded)
- Flow rate equations:

$$ideal\ gas: \frac{dm}{dt} = C_d\, A_{ou}\, P_{st} \sqrt{\frac{\gamma M_w}{RT_{st}}\left(\frac{2}{\gamma+1}\right)^{\frac{\gamma+1}{\gamma-1}}} \quad , \quad if\ \frac{P_{st}}{P_a} \geq \left(\frac{2}{\gamma+1}\right)^{-\frac{\gamma}{\gamma-1}} \qquad (choked\ \ flow)$$

$$\frac{dm}{dt} = C_d\, A_{ou}\, P_{st} \sqrt{\frac{2\gamma M_w}{(\gamma-1)RT_{st}}\left[\left(\frac{P_a}{P_{st}}\right)^{\frac{2}{\gamma}} - \left(\frac{P_a}{P_{st}}\right)^{\frac{\gamma+1}{\gamma}}\right]} \quad , \quad if\ \frac{P_{st}}{P_a} < \left(\frac{2}{\gamma+1}\right)^{-\frac{\gamma}{\gamma-1}} \qquad (unchoked\ flow)$$

3.2.3 Non-steady, isentropic ideal gas flow

Sallet and Palmer considers isentropic expansion and the relevant formulas can be derived and are as follows[6], valid for choked flow:

$$Q(t) = \frac{C_D A_o P_{st}(0)}{\sqrt{ZR^* T_{st}(0)}} K_1 F(t)^{(\gamma+1)/(\gamma-1)}, \tag{19}$$

$$P_{st}(t) = P_{st}(0) F(t)^{2\gamma/(\gamma-1)}, \tag{20}$$

$$T_{st}(t) = T_{st}(0) F(t)^2, \tag{21}$$

and

$$\rho(t) = \rho(0) F(t)^{2/(\gamma-1)}, \tag{22}$$

where

$$F(t) = \frac{1}{C_D A_o K_3 \sqrt{T_{st}(0)}\; t + 1}, \tag{23}$$

$$K_1 = \sqrt{\gamma \left(\frac{2}{\gamma+1} \right)^{\frac{\gamma+1}{\gamma-1}}}, \tag{24}$$

and

$$K_3 = \frac{\gamma-1}{2} \sqrt{ZR^* \gamma \left(\frac{2}{\gamma+1} \right)^{\frac{\gamma+1}{\gamma-1}}}. \tag{25}$$

There is also an expression for the duration of choked flow, namely

$$t_c = \frac{V}{C_D A_o K_3 \sqrt{T_{st}(0)}} \left\{ \left(\frac{2}{\gamma+1} \right)^{\frac{\gamma}{\gamma-1}} \frac{P_{st}(0)}{P_a} \right\}^{\frac{\gamma-1}{2\gamma}}, \tag{26}$$

after which the flow will be un-choked. Finally, the total mass of gas in the tank at any time is given by

$$M(t) = M(0)\, F(t)^{2/(\gamma-1)}. \tag{27}$$

3.3 Orifice Model

3.3.1 Method

Cases

A pressurised vessel with air is chosen for verification purposes as air is known to follow ideal gas behaviour closely. The expressions used to calculate the analytical results are only valid for choked flows, and the time axis is therefore cut-off when the choked flow ends.

Relevant data:

- Initial storage pressure: $40 \cdot 10^5$ Pa (40 bar)
- Initial storage temperature: 323.15 K
- Initial mass of air: 8619.85 kg
- Tank volume: 200 m^3
- Orifice diameter: 0.1 m
- Discharge coefficient: 0.88
- Ambient pressure: 101325 Pa
- Compressibility factor: 1
- Molecular weight for air: 28.95 kg/kmol

The above data was input both to the analytical formulas as well as the TVDI model. Note that the TVDI model does not take tank volume as input – rather it calculates the gas volume through an equation of state based on the initial mass, pressure and temperature. Since the equation of state is different from the ideal gas law used in the analytical computations, the initial gas volume in TVDI may differ from the analytical one – in fact the initial gas volume in TVDI in this case is 201.10 m^3, a rather insignificant deviation of 0.55%.

	Initial values		**Final values**	
	Analytical	**TVDI**	**Analytical**	**TVDI 40 / 400 steps**
Time (s)	0	0	526.2	534.8 / 526.2
Flow rate (kg/s)	62.14	62.79	0	0 / 0.08
Mass in vessel (kg)	8619.85022	8619.850586	624.1	650.8 / 650.9
Volume (m^3)	200.00	201.10	200.00	201.10 / 201.10
Pressure (Pa)	4000000	400000	101325	101325.9 / 101345.6
Temperature (K)	323.15	323.15	113.1	110.7 / 110.7

Table 7: Comparison of analytical and TVDI predicted results

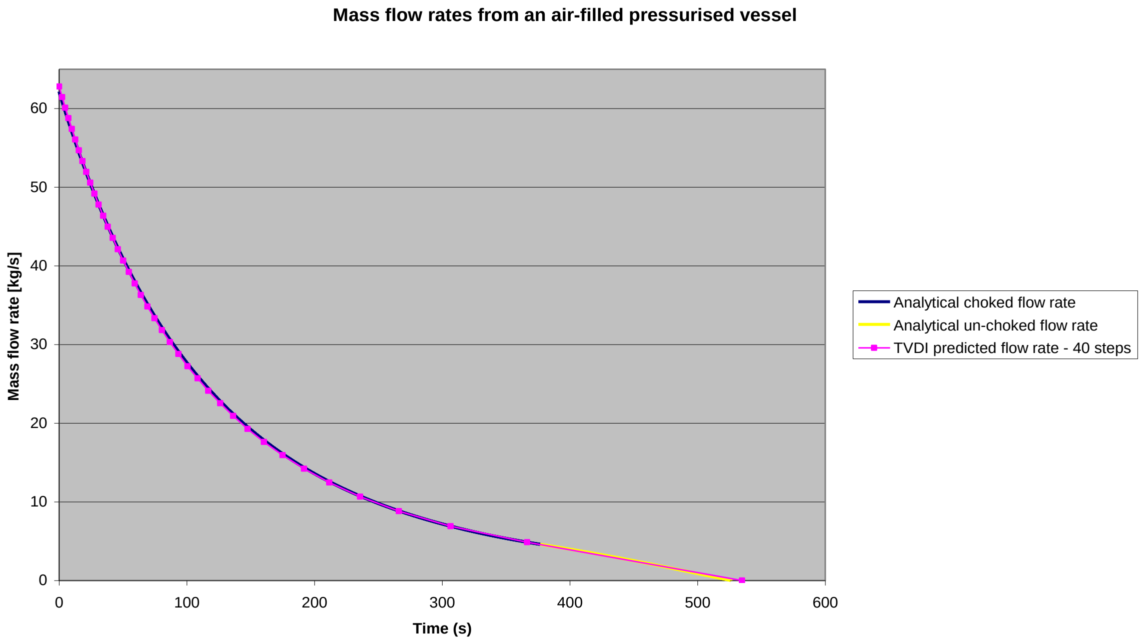

Figure 15: Comparison of flow rates for a pressurised gas vessel

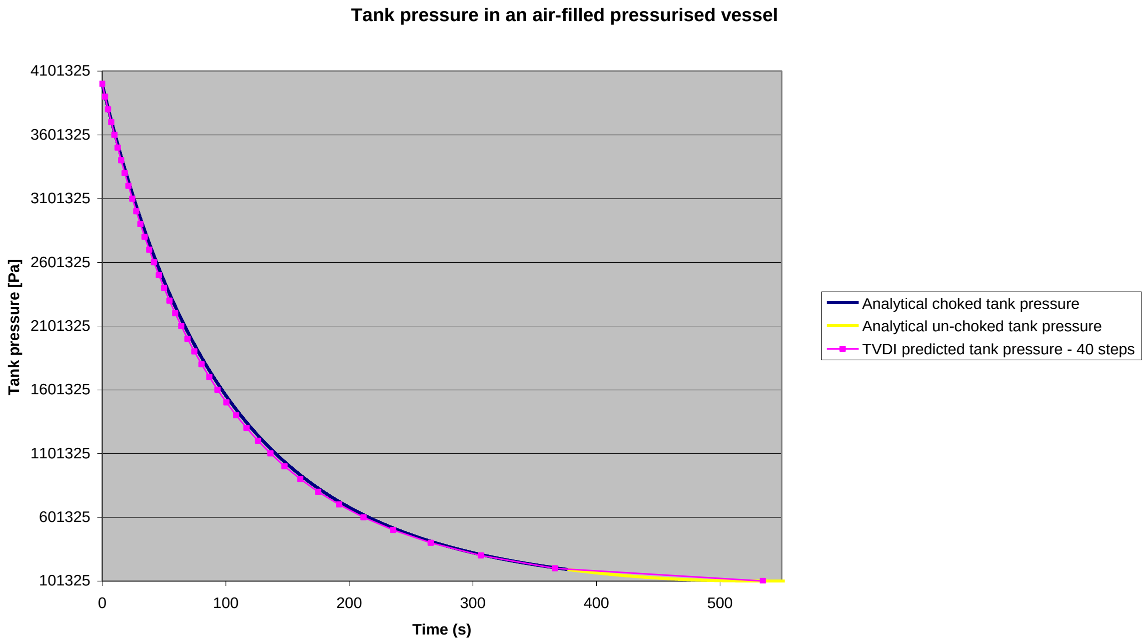

Figure 16: Comparison of tank pressures for a pressurised gas vessel

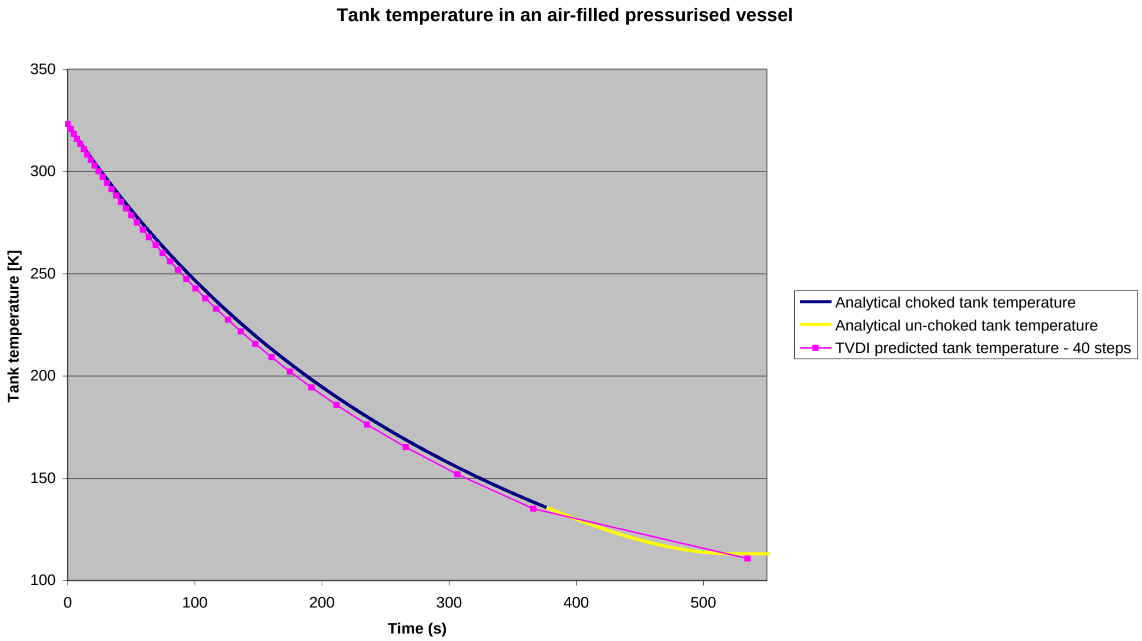

Figure 17: Comparison of tank temperatures for a pressurised gas vessel

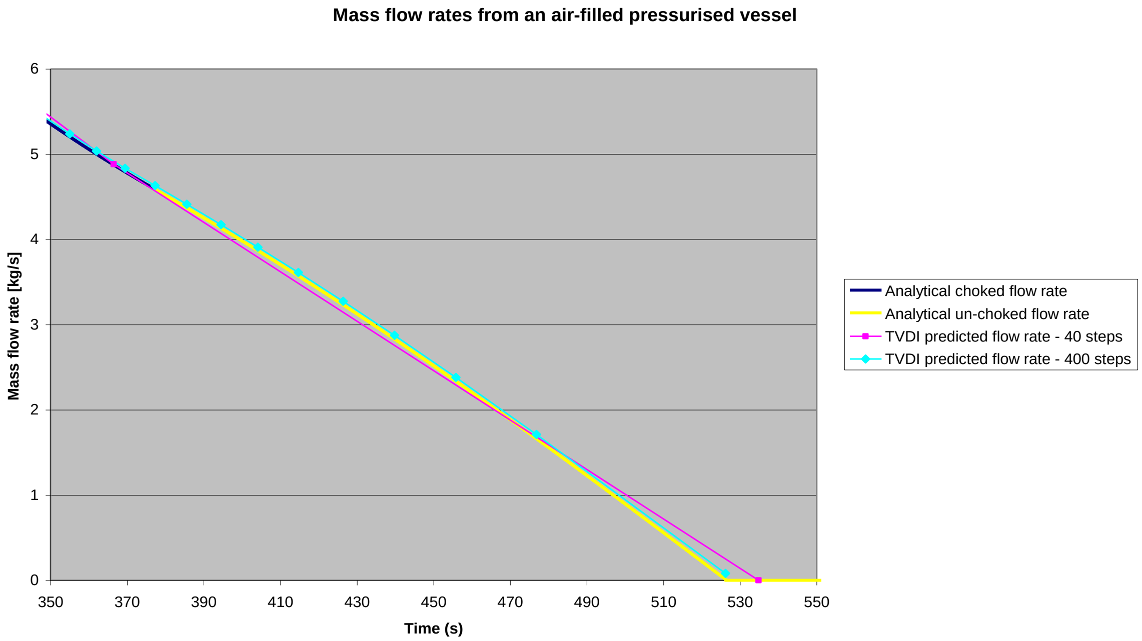

Figure 18: Comparison of flow rates for un-choked flow

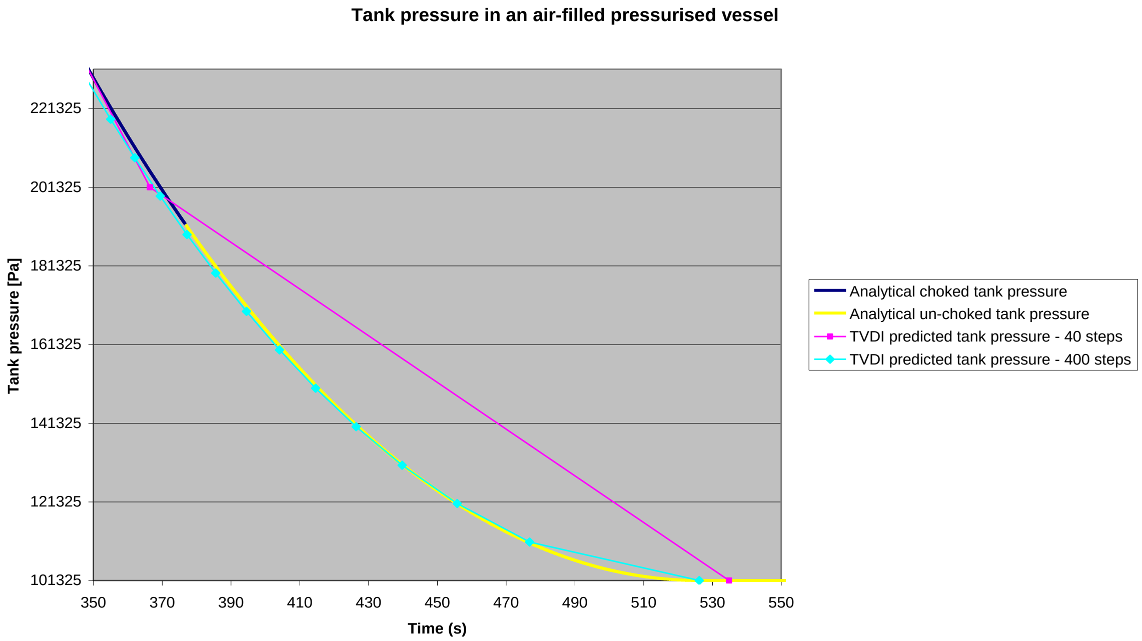

Figure 19: Comparison of tank pressures for un-choked flow

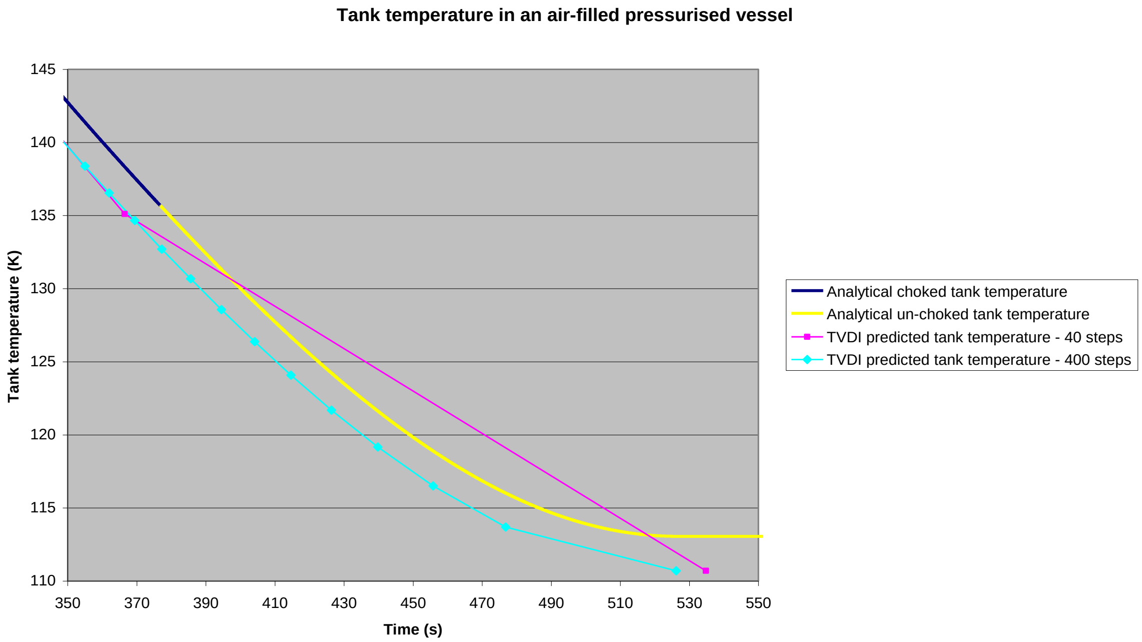

Figure 20: Comparison of tank temperatures for un-choked flow

3.3.2 Findings

Comparison of analytical and TVDI predicted mass flow rates, tank pressure and tank temperature can be found in Figure 15, Figure 16 and Figure 17, respectively. The mass flow rates appear to almost completely coincide, and the tank pressures are also very close, though TVDI seems to predict marginally lower pressures. The tank temperatures are also very close, though the difference is here a bit more pronounced – the TVDI temperatures are slightly smaller than the analytical ones.

The default number of time steps in TVDI is 40. These steps are based on equal pressure decrements, and therefore there are in this case only two steps in the un-choked flow regime. This is clearly not sufficient for a meaningful comparison with analytical results, and TVDI was therefore run again with an increased number of steps – 400. These results can be found in Figure 18, Figure 19 and Figure 20, focusing on the un-choked flow regime. Again, there is extremely good agreement for flow rates and tank pressures, whereas the trend of TVDI slightly under-predicting the tank temperature compared to analytical results is still present.

Further, looking at
Table 7, there is generally very good agreement of results. However, the analytical model discharges roughly 4% more mass than what is predicted by TVDI.

List of issues:

- Why is the temperature slightly 'under-predicted' by TVDI?
- Why does the analytical model discharge 4% more mass?
- Could the issue of ideal vs non-ideal gas possibly answer the above questions?

4. VALIDATION

4.1 Introduction

Previous validation work on TVDI is reported later in this section, whereas new validation work is reported in subsequent sections.

Assessment of the pure gas release model TVRGAS for pressurized mixtures of light hydrocarbons:

- Section 4.2: Szczepanski
  - Validation against experimental results
- Section 4.3: Haque S9
  - Verification against numerical results (BLOWDOWN)
- Section 4.4: Haque S12
  - Verification against numerical results (BLOWDOWN)

Assessment of the multiphase release model TVLEAK, saturated mixtures of light hydrocarbons:

- Melhem – LPG Cylinder
  - Validation against experimental results and verification against numerical results (SuperChems).

4.1.1 Previous TVDI validation work

Duree[7] (Shell Research) carried out PHAST 4.2 validation against hydrocarbon experiments of by Shell and Imperial College. This included blowdown for pressurised gaseous methane/ethane/propane mix – experiments by Imperial College (Haque et al.[8];Fig. 2.3)

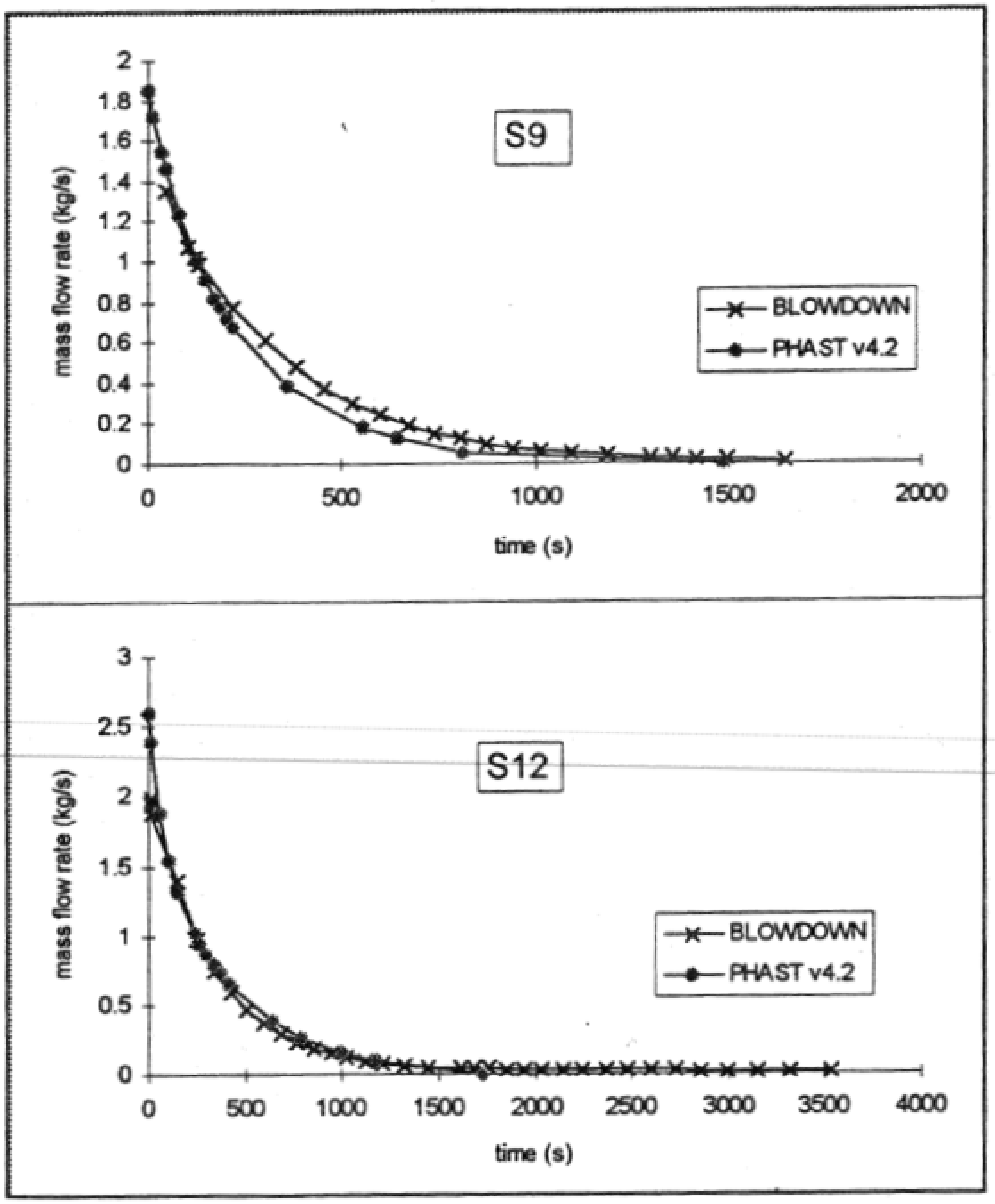

Figure 2.3 Comparison of mass flow rate predictions vs. time (Data Set 1.3)

Figure 21. PHAST4.2 validation for blowdown of pressurised gaseous methane/ethane/propane vessel[iv]

[iv] Note that Richardson et al. carried out further extensive validation of 2-phase blowdown including heat transfer from the vessel. A DNV model has been developed for this by Svein Morud, and could be of consideration for this. TVDI does not include effect of heat transfer, and from this point 2-phase experimental data with a perfectly insulated vessel wall would be of interest. Future. To check the existence of these data.

4.1.2 SUPERCHEMS documentation

Table 6 and Figure 23 in the SUPERCHEMS overview Paper by Melhem and Fisher[9] show an example of a gas propane cylinder blowdown (experimental data; TVDI validation for gas) based on experimental by Melhem et al.(1991)[10]. Experimental results as a function of time for the cylinder pressure and the cylinder mass are compared with SUPERCHEMS[v]. There are further validation examples given in this paper but they correspond to scenarios which appear not be able to be run by PHAST (e.g. using multiple piping to vessels, etc.).

TABLE 6. Propane Cylinder Experimental Data Summary

Variable	Value
Cylinder weight (empty) (kg)	30.4
Cylinder volume (m^3)	0.102
Cylinder charge (kg)	43.7
Initial temperature (K)	308
Initial pressure (bar)	16
Propane mole fraction	97.3
Butane mole fraction	1.7
Other	1.0
Release orifice size (in)	3/8 ID
Release piping (ft)	50 (copper tubing)
Copper roughness (m)	0.0000457 (assumed)
Ambient temperature (F)	103
Relative humidity (percent)	95
Date	July 15, 1991 at 2:00 pm
Flow phase	Gas flow only
Total mass vented (kg)	8.0 in 180 s

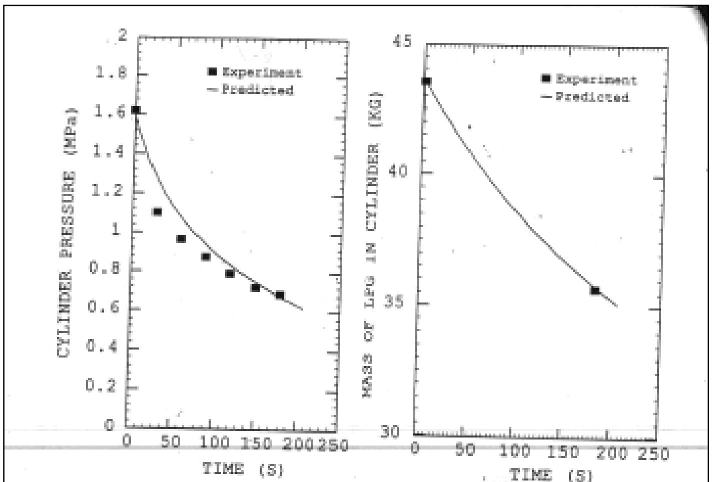

FIGURE 23 Propane cylinder blowdown: comparison of experimental data and model predictions for pressure profile and total mass vented.

Figure 22. SUPERCHEMS validation for pressurised gaseous propane vessel

4.1.3 Previous recommendations for further validation

1. Redo Shell's validation for vessel blowdown (Figure 21)
2. Validation against Melhem experiment for propane vessel blowdown (Figure 22)
3. TVDI data against 2-phase blowdown (data to be identified)

4.2 Szczepanski

This experiment was reported in a publication by Szczepanski[11] and also later by Oke[12]. The experimental data used here is taken from the latter publication.

4.2.1 Vessel geometry

- The vessel is a vertical cylinder with dome-shaped ends
- Tan-to-tan height of vessel: 2.75 m
- Internal diameter: 1.13 m
- Estimated overall height: 3.24 m
- End thickness: 0.05 m
- Wall thickness: 0.059 m
- Orifice diameter: 0.01 m
- Orifice gas discharge coefficient: 0.86
- Interior dome / spherical cap height: 0.195 m

[v] There appears to be discrepancies about the experimental set up reported in the original paper from 1993[10] and the SuperChems paper from 1997[9]. Until this is clarified, this experiment cannot be used for validation purposes.

- Interior dome / spherical cap radius: 0.565 m
- Interior vessel volume:
  - Cylinder + 2*dome = $3.1415*0.565^2*2.75$ m^3 + $2*3.1415/6*0.195*(3*0.565^2+0.195^2)$ m^3 = 2.9611 m^3.

4.2.2 Inventory and storage conditions

- The material is a hydro-carbon mixture with the following mole fraction composition:
  - Methane: 0.64
  - Ethane: 0.06
  - Propane: 0.285
  - n-Butane: 0.015
- Vessel temperature: 293 K
- Vessel pressure (absolute): 118 bar = 116.45 atm

4.2.3 Notes on input to the model spreadsheet

- The above mixture was created as a pseudo-component mixture in Phast 6.54 and exported to use with the TVDI spreadsheet. The vapour density at initial stagnation conditions was calculated in Phast to be 248.101 kg/m^3. With a tank volume of 2.9611 m^3, this gives an initial material mass of 734.7 kg.
- Cylinders with dome-shaped ends are currently not supported in TVDI, so an equivalent vertical cylinder (same diameter and volume) was used, with a height of 2.9527 m.

4.2.4 Results

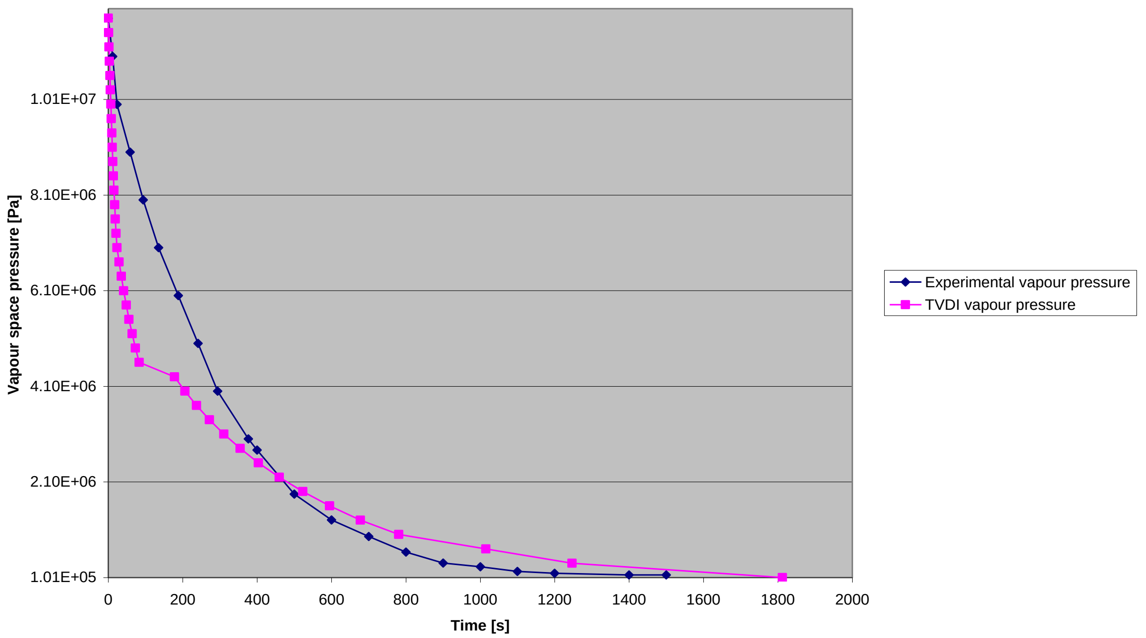

Figure 23: Vapour space pressure – experimental results (Szczepanski[11]) vs TVDI predictions

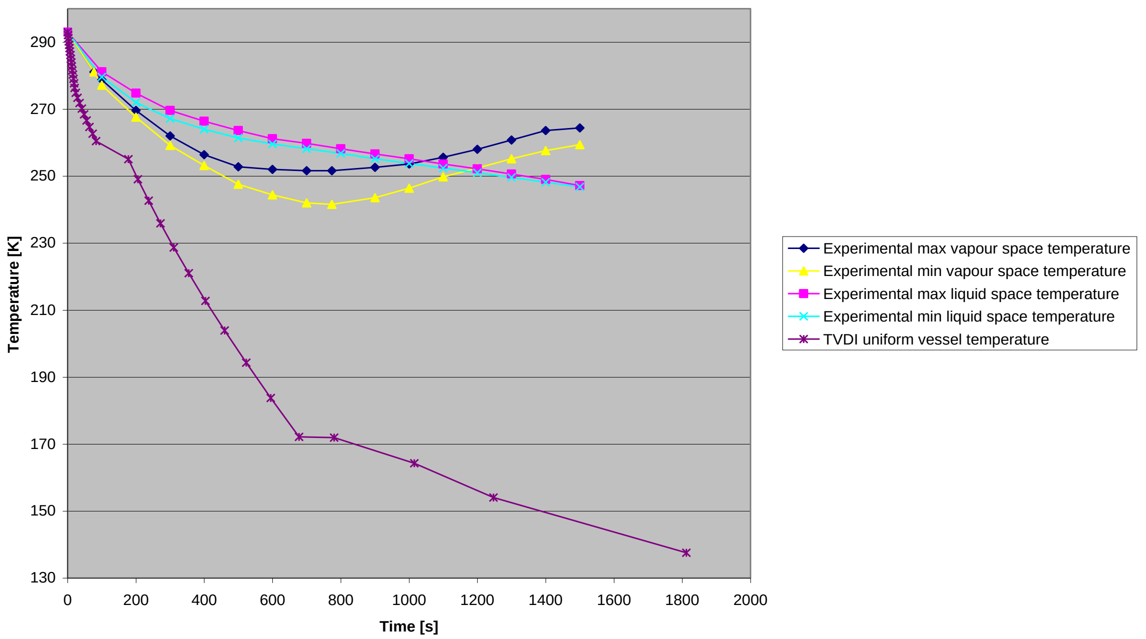

Figure 24: Temperatures – experimental results (Szczepanski) vs TVDI predictions

4.2.5 Findings

Before comparing the results, it should be noted that the usage of a pseudo-component mixture in place of a multi-component mixture is very crude. Initially the pseudo-component mixture is a pressurised gas, meaning that it is the TVRGAS submodel that is deployed.

Figure 23 reveals that the TVDI pressure initially drops far more rapidly than what was observed experimentally. Also note that there is a 'kink' in the pressure curve just before 200 s is reached. This coincides with the transition past the critical point (45 bar, 252 K).

Figure 24 shows that the temperature[vi] predicted by TVDI keeps dropping and dropping, while the temperature measured experimentally drops far less. It is thought that the TVDI results deviate so much due the use of a pseudo-component mixture and also due to the fact that no phase-changes are taken into account in the TVRGAS submodel, and heat transfer from the walls are also ignored.

4.3 Haque – S9

This experiment was reported and labelled *S9* by Haque et al[8].

4.3.1 Vessel geometry

The geometry is the same as in the Szczepanski case. A discharge coefficient of 0.86 is thus applied, but there is no information in Haque to confirm this value.

4.3.2 Inventory and storage conditions

- The material is a hydro-carbon mixture with the following mole fraction composition:
  - Methane: 0.855
  - Ethane: 0.045
  - Propane: 0.100
- Vessel temperature: 303 K
- Vessel pressure: 120 bara = 118.431 atm = 1.20e7 Pa.

4.3.3 Notes on input to the model spreadsheet

- The mixture was created in Phast 6.54 using pseudo-component logic and exported to use with the TVDI spreadsheet. The vapour density at initial stagnation conditions was calculated in Phast to be 121.87 kg/m^3. With a tank volume of 2.9611 m^3 this gives an initial material mass of 360.9 kg.

[vi] The temperature predicted by TVDI drops so low that it reaches its saturation temperature at the four last time steps. The model reports liquid fraction rather than temperature for these time steps, so the temperature at these steps was obtained by using Phast to find the saturation temperature at the corresponding pressures.

4.3.4 Results

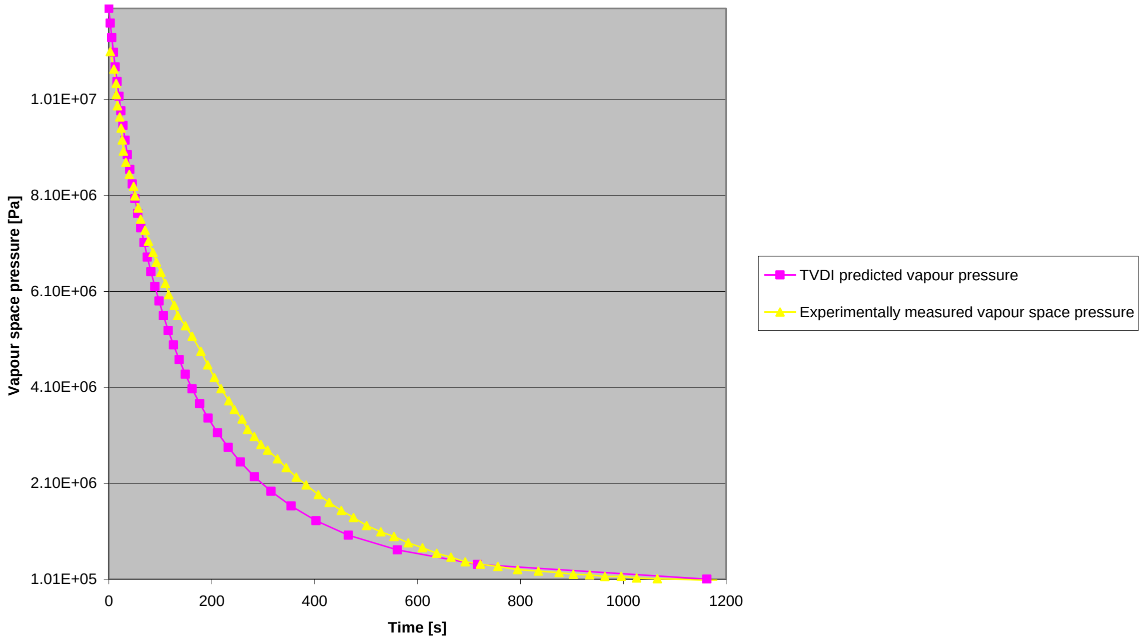

Figure 25: Vapour space pressure case S9 –experiment vs TVDI predictions

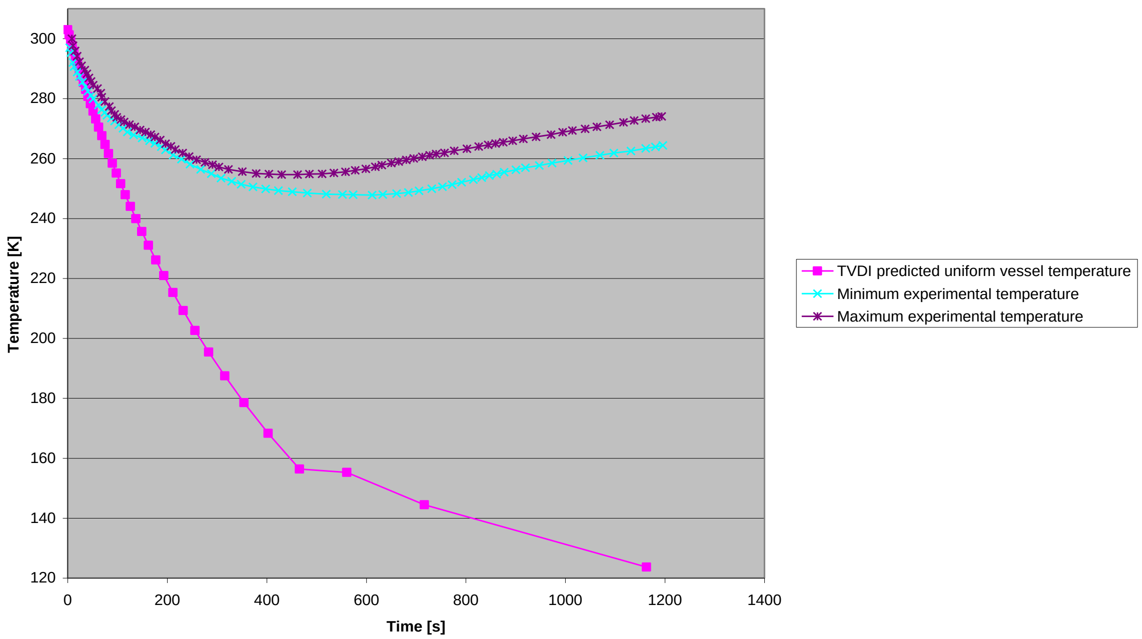

Figure 26: Temperatures case S9 – experiment vs TVDI predictions

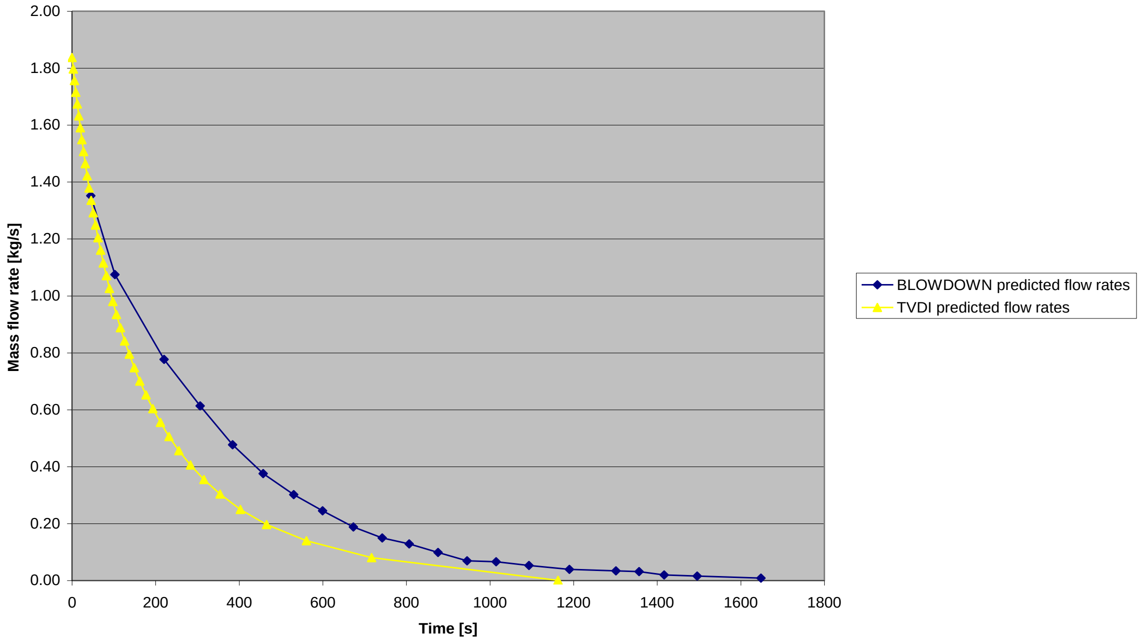

Figure 27: Mass flow rates case S9 – BLOWDOWN and TVDI predictions

4.3.5 Findings

Findings from the Szczepanski case generally apply to this case as well.

The pressure predictions are fairly good as seen in Figure 25, but Figure 26 shows that the temperature predictions are again way too low. Note that flow rates in Figure 27 compare TVDI and the BLOWDOWN[13] model as experimentally measured flow rates are not available. It is expected that the flow rate predicted by BLOWDOWN is fairly accurate since BLOWDOWN predicts the vapour space pressure and temperatures well. We observe that the TVDI flow rate is too low but follows a similar trend, with a maximum deviation of about 50% after 400 s.

4.4 Haque – S12

This experiment was reported and labelled *S12* by Haque et al.[8].

4.4.1 Vessel geometry

The geometry is the same as in the Szczepanski case. A discharge coefficient of 0.86 is thus applied, but there is no information in Haque to confirm this value.

4.4.2 Inventory and storage conditions

- The material is a hydro-carbon mixture with the following mole fraction composition:
    - Methane: 0.665
    - Ethane: 0.035
    - Propane: 0.300
- Vessel temperature: 293 K
- Vessel pressure: 120 bara = 118.431 atm = 1.20e7 Pa.

4.4.3 Notes on input to the model spreadsheet

- The mixture was created in Phast using pseudo-component logic and exported to use with the TVDI spreadsheet. The vapour density at initial stagnation conditions was calculated in Phast to be 237.672 kg/m^3. With a tank volume of 2.9611 m^3 this gives an initial material mass of 703.8 kg.

4.4.4 Results

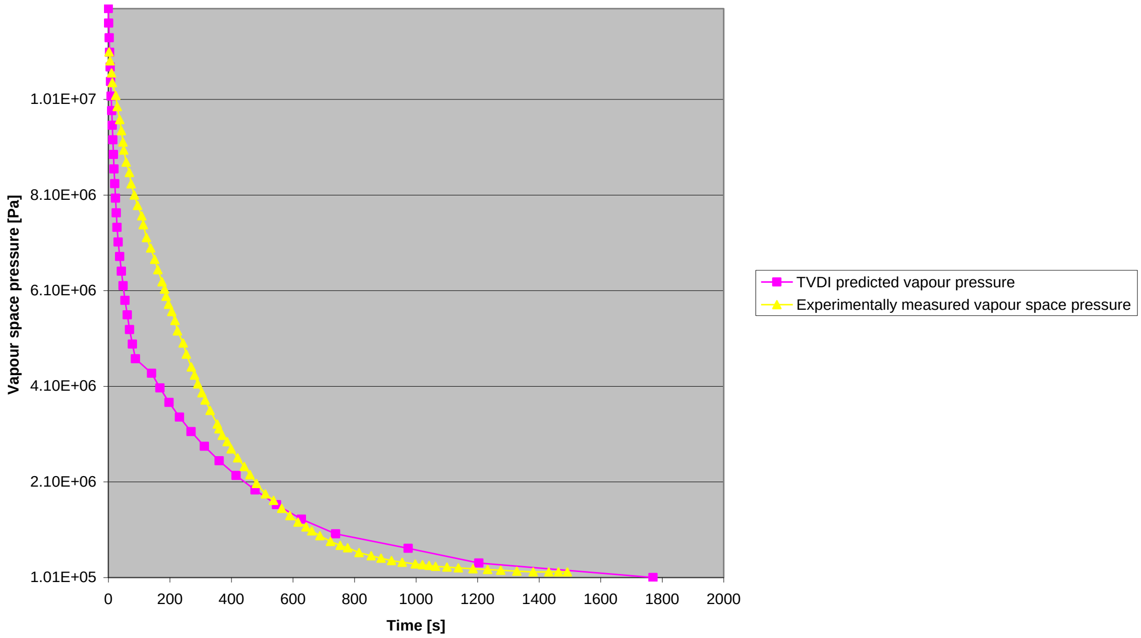

Figure 28: Vapour space pressure case S12 – experiment vs TVDI predictions

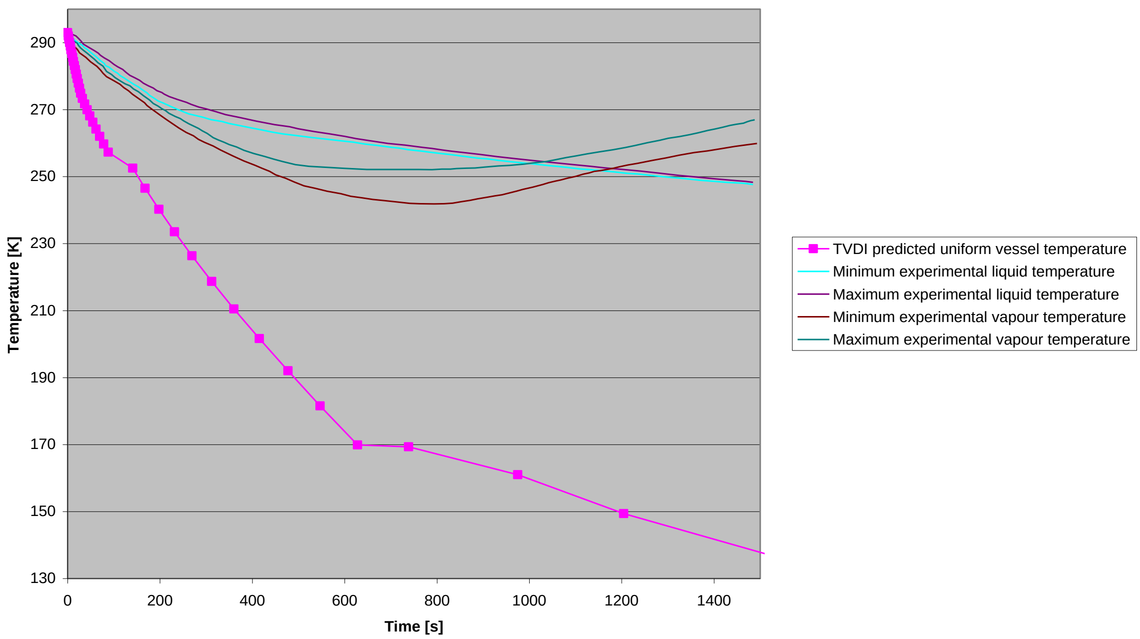

Figure 29: Temperatures case S12 – experiment vs TVDI predictions

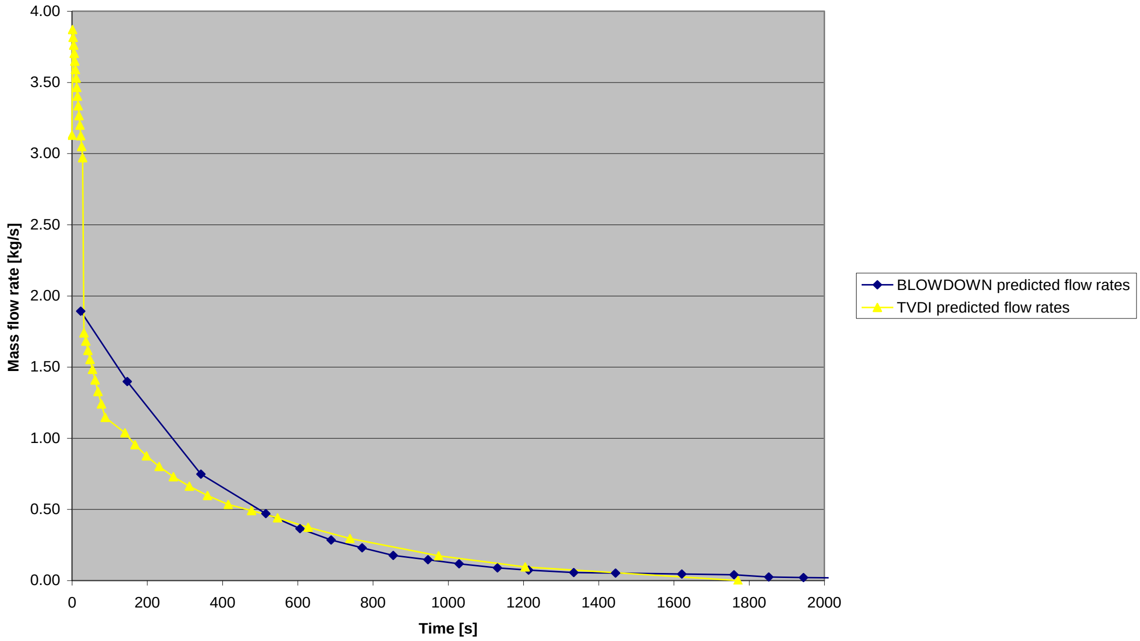

Figure 30: Mass flow rates case S12 – BLOWDOWN and TVDI predictions

4.4.5 Findings

Looking at **Figure 28** and **Figure 29** one may conclude that the previous findings from the Szczepanski case in Section 04.2.4 generally apply to this case as well. In particular note that all the TVDI predicted results have a 'kink' shortly after 100 s – this is again probably due to difficulties near the critical point of the pseudo-component mixture (45 bar, 248.4K). Other trends are similar to those observed for the S9 case reported above, though the flow rate comparison in **Figure 30** shows better agreement between BLOWDOWN and TVDI than for case S9.

4.5 Melhem – LPG Cylinder

This experiment was reported in a paper by Melhem and Fisher[9], and the experimental results are taken from this paper - see Table 6 and the Section "LPG Cylinder Blowdown".

4.5.1 Vessel geometry

- Cylinder volume: 0.102 m^3
- Release orifice diameter: 0.009525 m
- Length of attached pipe: 15.24 m
- Ratio of pipe length to pipe diameter[vii]: 1600
- Pipe roughness length: 0.0000457 m

4.5.2 Inventory and storage conditions

- Total inventory mass: 43.7 kg
- Material composition in mole fractions:
  - Propane: 0.973
  - Butane: 0.017

[vii] Note that this ratio of length to diameter is large enough to constitute a long pipe while the model strictly speaking supports the attachment of short pipes only.

- Other: 0.01
- Initial temperature: 308 K
- Initial pressure: 16 bar = 1600000 Pa
- Ambient temperature: 312.5944 K
- Ambient humidity: 0.95

4.5.3 Notes on input to the model spreadsheet

- A pseudo-component mixture was created using Phast 6.54 with the composition given above; 'other' was here chosen to be methane.
- It is assumed that the inventory in the experiment was at saturated conditions. The pseudo-component mixture created in Phast, however, is not exactly saturated at the experimental storage conditions. In the model, the pressure was kept the same as in the experiment, while the temperature was adjusted to reach saturated conditions at 312 K (4 K above experimental value).
- Suggested cylinder dimensions with volume 0.102 m^3:
  - Diameter: 0.4 m
  - Height: 0.812 m
  - Cylinder oriented vertically.
- Note that the dimensions of the vessel used in the experiments are unknown – only the volume is known. As such a somewhat arbitrary diameter and height was chosen above, yielding the correct volume. However, the cross-sectional area of the tank and hence the liquid surface, may deviate from the one in the experiment, and this will in turn influence evaporation/condensation rates in TVDI.
- It is reported that only gas was released in the experiment. We have therefore attached the pipe towards the top of the cylinder so as to only model the evacuation of vapour and not liquid.

4.5.4 Results

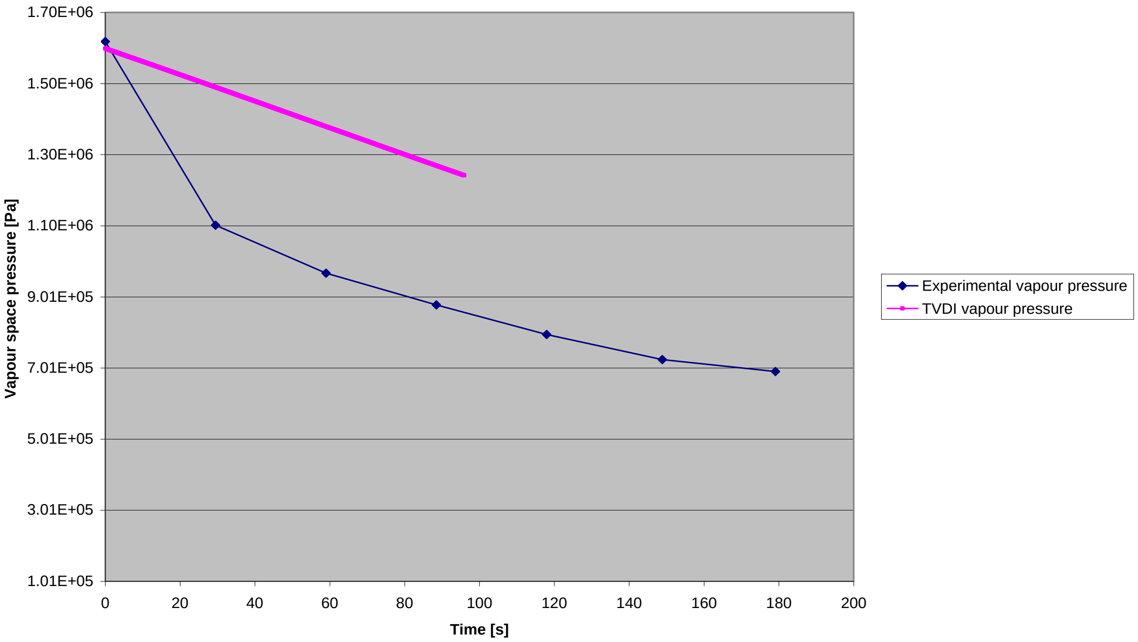

Figure 31: Vapour space pressures comparison - experiments and TVDI.

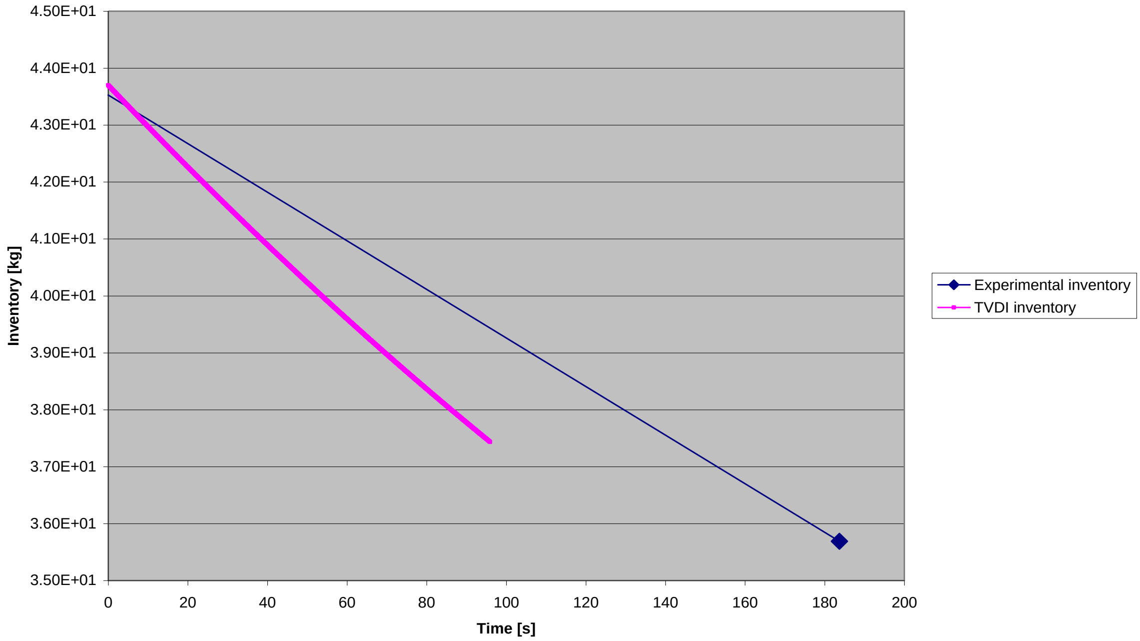

Figure 32: Inventory comparison - experiments and TVDI.

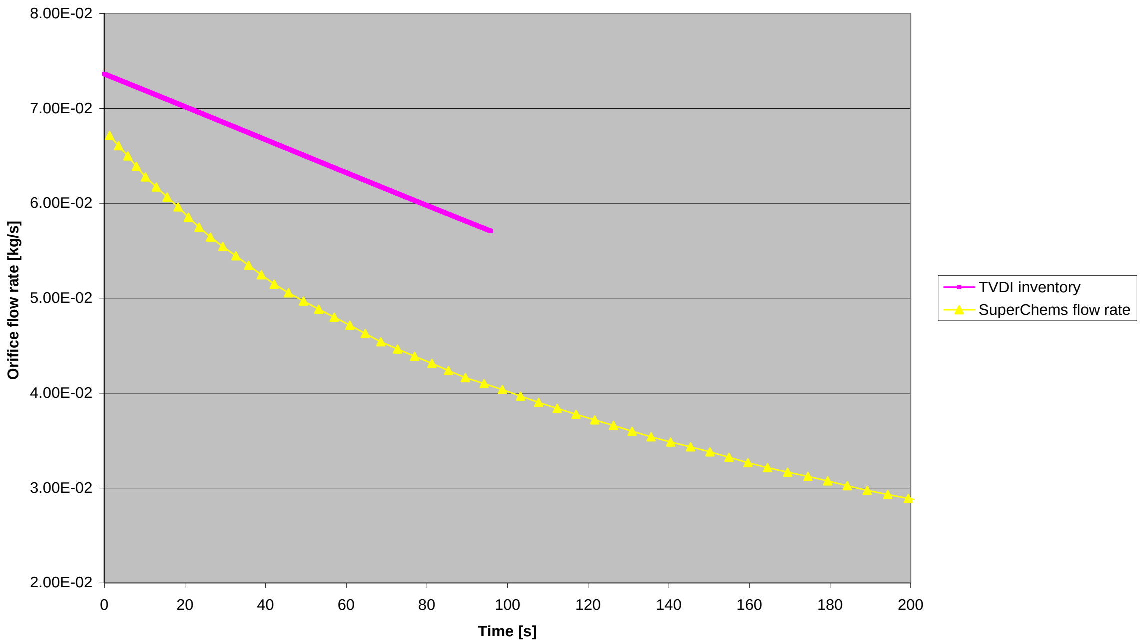

Figure 33: Flow rate comparison - SuperChems and TVDI.

4.5.5 Findings

Before discussing the results, it should be noted that the current scenario is beyond the scope of the current modelling capabilities in TVDI. The reason for this is the very large pipe length to diameter ratio of 1600. Such a large ratio corresponds to the long pipeline models in Phast, but these models do not support having a vessel attached at one end. This blow-down scenario has still been included here to highlight the current limitation in TVDI and also to serve as a possible benchmark in the future for an extended TVDI model.

When looking at the TVDI results in Figure 31 to Figure 33, one notice the premature termination after about 95 s. The termination is due to TVDI having exceeded the maximum number of steps allowed (1000) as it encounters certain numerical problems.

Figure 31 shows that TVDI does not predict the initial drop in vapour space pressure as observed experimentally. The higher vapour space pressure would lead to a higher discharge rate and thus lower inventory as can be seen in Figure 32. The discharge rates were not measured experimentally, but a comparison of predictions between SuperChems and TVDI in Figure 33 shows that the TVDI values are larger.

APPENDICES

Appendix A. Future verification – combined liquid leak and vapour space blowdown

A.1 Introduction

The TVDI model can currently not account for a man-initiated controlled blowdown as a measure to reduce the impact of an ongoing accidental release. However, the modelling of such a scenario is one of the main priorities when TVDI is further developed, and as such we here look at such a blowdown scenario that can be used for verification purposes in the future.

A.2 A liquid leak with vapour space blowdown

We will here consider a pressurised vessel containing an ideal gas in the top space and an incompressible liquid in the bottom space. There is an accidental orifice leak in the liquid space with area A_L and a controlled blowdown through an orifice of area A_G in the vapour space. For simplicity we here consider a vessel in the shape of a rectangular box with constant cross-sectional area A, length L_{tank}, width W_{tank} and height H_{tank}.

The situation is made as simple as possible and includes the following assumptions:

- Gas:
  - Ideal
  - Isentropic expansion
  - No condensation
- Liquid:
  - Incompressible
  - No evaporation
- No heat transfer between phases or fluids/vessel
- Cuboidal vessel with constant cross-section area

See Figure 34 for a schematic over of the scenario.

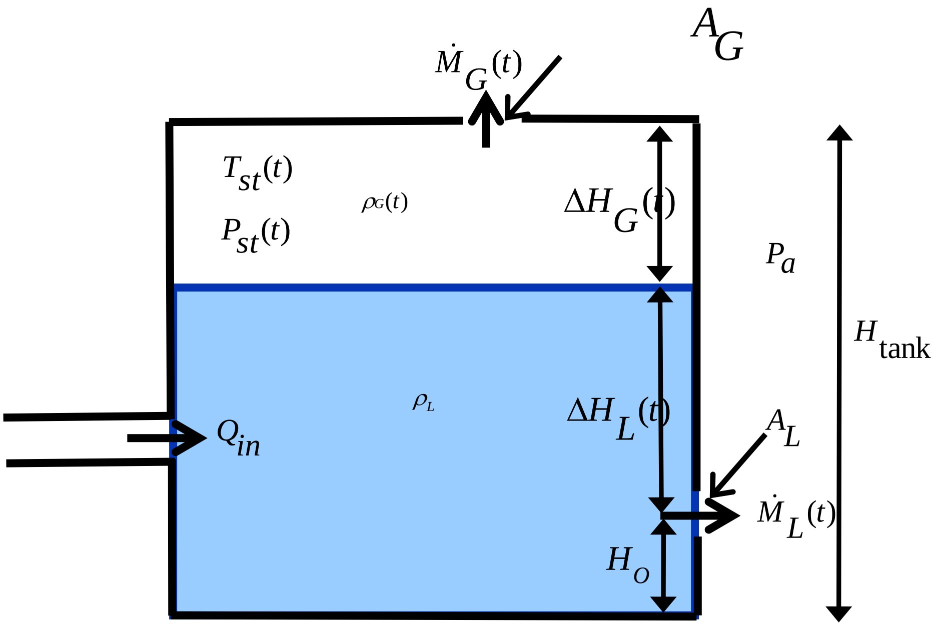

Figure 34: Schematic overview of a liquid leak - vapour space blowdown scenario with inflow.

A.2.1 MASS FLOW RATE OF GAS

Using isentropic relationship, the flow rate of gas can be expressed as (see e.g. Sallet and Palmer[6]):

$$\dot{M}_G(t) = -\frac{C_{DG} A_G P_{st}(t)}{\sqrt{R/M_W \, T_{st}(t)}} \sqrt{\frac{2\gamma}{\gamma-1}\left[\left(\frac{P_a}{P_{st}(t)}\right)^{\frac{2}{\gamma}} - \left(\frac{P_a}{P_{st}(t)}\right)^{\frac{\gamma+1}{\gamma}}\right]} \, . \qquad \textbf{(28)}$$

Assuming an isentropic gas expansion, we can express the pressure and temperature in terms of the height and mass of gas:

$$P_{st}(t) = P_{st}(0)\; r(t)^{\gamma} \qquad \textbf{(29)}$$

and

$$T_{st}(t) = T_{st}(0)\; r(t)^{\gamma-1} \, , \qquad \textbf{(30)}$$

where

$$r(t) = \left(\frac{\Delta H_G(0)}{\Delta H_G(t)}\right)\left(\frac{M_G(t)}{M_G(0)}\right) . \qquad \textbf{(31)}$$

We may therefore get

$$\dot{M}_G(t) = -\frac{C_{DG} A_G P_{st}(0)}{\sqrt{R/M_W \, T_{st}(0)}}\; r(t)^{\frac{1}{2}(\gamma+1)} \cdot \sqrt{\frac{2\gamma}{\gamma-1}\left[\left(\frac{P_a}{P_{st}(0)}\right)^{\frac{2}{\gamma}}\left(\frac{1}{r(t)}\right)^{2} - \left(\frac{P_a}{P_{st}(0)}\right)^{\frac{\gamma+1}{\gamma}}\left(\frac{1}{r(t)}\right)^{\gamma+1}\right]} \, . \qquad \textbf{(32)}$$

The above expression is for unchoked flow. The flow is choked if

$$\frac{P_{st}(t)}{P_a} \geq \left(\frac{2}{\gamma+1}\right)^{-\frac{\gamma}{\gamma-1}} , \qquad \textbf{(33)}$$

and the mass flow rate equation is then given by

$$\dot{M}_G(t) = -\frac{C_{DG} A_G P_{st}(0)}{\sqrt{R/M_W \, T_{st}(0)}}\; r(t)^{\frac{1}{2}(\gamma+1)} \sqrt{\gamma\left(\frac{2}{\gamma+1}\right)^{\left(\frac{\gamma+1}{\gamma-1}\right)}} \, . \qquad \textbf{(34)}$$

A.2.2 MASS FLOW RATE OF LIQUID WITHOUT INFLOW

We find the mass flow rate of liquid through solving a differential equation for the liquid height as described in Section 0:

$$\frac{d(\Delta H_L(t))}{dt} = -C_{DL}\,\frac{A_L}{A}\sqrt{2\left(\frac{P_{st}(0)\; r(t)^{\gamma} - P_a}{\rho_L} + g\Delta H_L(t)\right)} \qquad \textbf{(35)}$$

Also note that

$$\Delta H_G(t) = H_{\text{tank}} - H_O - \Delta H_L(t)\,, \qquad \textbf{(36)}$$

so effectively we have a coupled set of two non-linear differential equations in two unknowns: mass flow rate of gas $\dot{M}_G(t)$ and liquid head ΔH_{L}. The mass flow rate of liquid $\dot{M}_L(t)$ may subsequently be obtained from Equation (3).

A.2.3 PUMPED INFLOW

Assuming that there is a pumped liquid inflow Q_{in}, this will contribute towards increasing the height of liquid in the tank:

$$Q_{in} = \frac{d(\rho_L V_{in})}{dt} = \frac{d(\rho_L AH)}{dt} = \rho_L A \frac{dH}{dt} = \rho_L A \frac{d(\Delta H_L)}{dt} \Rightarrow \frac{d(\Delta H_L)}{dt} = \frac{Q_{in}}{\rho_L A} \qquad \textbf{(37)}$$

,

The differential equation for liquid height may therefore be modified to account for the inflow:

$$\frac{d(\Delta H_L(t))}{dt} = -C_{DL}\,\frac{A_L}{A}\sqrt{2\left(\frac{P_{st}(0)\;r(t)^{\gamma} - P_a}{\rho_L} + g\Delta H_L(t)\right)} + \frac{Q_{in}}{\rho_L A} \qquad \textbf{(38)}$$

A.2.4 VERIFICATION CASES

Some cases with air and water have been considered and the relevant equations presented above have been solved numerically in an Excel spreadsheet. The results are not included at this stage but will likely be included when the TVDI model has been extended to take into account inflow and/or vapour space blowdown.ous

About DNV

We are the independent expert in risk management and quality assurance. Driven by our purpose, to safeguard life, property and the environment, we empower our customers and their stakeholders with facts and reliable insights so that critical decisions can be made with confidence. As a trusted voice for many of the world's most successful organizations, we use our knowledge to advance safety and performance, set industry benchmarks, and inspire and invent solutions to tackle global transformations.

Digital Solutions

DNV is a world-leading provider of digital solutions and software applications with focus on the energy, maritime and healthcare markets. Our solutions are used worldwide to manage risk and performance for wind turbines, electric grids, pipelines, processing plants, offshore structures, ships, and more. Supported by our domain knowledge and Veracity assurance platform, we enable companies to digitize and manage business critical activities in a sustainable, cost-efficient, safe and secure way.

DNV | digital@dnv.com | dnv.com/digital

REFERENCES

[1] Witlox, H.W.M., Harper, M., and Fernandez, M., "UDM validation document", UDM Technical Reference Manual, DNV (2017)

[2] Lees, F.P., "Loss Prevention in the process industries: hazard identification, assessment and control", Second Edition, Butterworth-Heinemann, Oxford (1996), , Volume 1, Sections 15.1 until 15.9 (pp. 15.1-57)

[3] Committee for the Prevention of Disasters, "Methods for the calculation of physical effects - TNO Yellow Book, CPR14E, Third Edition, SDU (1997), Part I, Chapter 2 "Outflow and spray release" by van den Bosch, C.J.H. and Duijm, N.J.

[4] Hissong, D.W., "Effect of LNG Tank Shape on Release Rates", 11th Annual Symposium, Mary Kay O'Conner Process Safety Center, Texas A&M University, Texas. (October 28-29, 2008)

[5] Crowl, D.A., "Liquid discharge from process and storage vessels", J. Loss. Prev. Process Ind., Vol 5, No 2, pp. 73 – 80 (1992)

[6] Sallet, D.W. and Palmer, M.E., "The Non-steady Flow of Gases and Vapours From Pressure Vessels", Proc. Insn. Mech. Engrs. Vol 194, pp. 225 – 230 (1980)

[7] Duree, P., "Model evaluation of the DNV Technica PHAST package", Draft Report TNER.95.***, Thornton Research Centre, Chester, UK (1995)

[8] Haque, M.A., Richardson, S.M., Saville, G., Chamberlain, G and Shirvill, L., "BLOWDOWN of Pressure Vessels II – Experimental validation of computer model and case studies", Trans. IChemE 70, Part B (1992)

[9] Melhem. G.A., and Fisher, H.G., "An overview of SuperChems for DIERS: a program for emergency relief system and effluent handling designs", Process Safety Progress 16 (3), pp. 185-197 (1997)

[10] Melhem, G.A., Croce, P.A., and Abraham, H. "Data Summary of the National Fire Protection Association's BLEVE Tests", Process Safety Progress 12 (2), pp. 76 – 82 (1993)

[11] Szczepanski, R., "Simulation programs for blowdown of pressure vessels", IChemE SONG Meeting (1994)

[12] Oke, A. "Modelling Liquid Space Blowdown", M.Sc. Thesis, University College London (2000)

[13] Haque, M.A., Richardson, S.M. and Saville, G. "BLOWDOWN of Pressure Vessels I – Computer Model", Trans. IChemE 70, Part B (1992)